These findings indicate that bioengineered tooth generation techniques can contribute to the rebuilding of a fully functional tooth.

Critical issues in tooth regenerative therapy are whether the bioengineered tooth can reconstitute functions such as mastication (32) and responsive potential to mechanical stress (31, 33) and noxious stimulations (34), including cooperation of the regenerated tooth with both the oral and maxillofacial regions. Eruption and occlusion are essential first steps toward dental organ replacement therapy and successful incorporation into the oral and maxillofacial region (21, 36). Our laboratory has demonstrated previously that a bioengineered tooth germ can develop into a tooth with the correct structure in an adult mouse (29). It has also been reported previously that normal tooth germ isolated from murine embryos and a bioengineered tooth constructed from cultured tooth bud cells can develop and erupt in a toothless oral soft tissue region (diastema) of adult mice and in the tooth extraction sockets of an adult rat (37–42). In our current study, we provide evidence that a bioengineered tooth with the same hardness as an adult natural tooth can erupt with normal gene expression, including *Csf1* and *Pthr1*, which are thought to regulate osteoclastogenesis, and achieve functional occlusion with the opposing natural teeth. Previous reports have suggested that the eruption of tooth germ is generally induced at the site of tooth development and by the gubernacular cord, which is derived from the epithelium of the dental lamina (43). Hence, our findings provide significant insights into tooth eruption mechanisms and strongly suggest that masticatory potential can be successfully restored by the transplantation of bioengineered tooth germ.

To establish cooperation between the bioengineered tooth and the maxillofacial region, 1 critical issue to address is whether a functional PDL is achieved and thereby the restoration of interactions between the bioengineered tooth and the alveolar bone (31, 33). The PDL has essential roles in tooth support, homeostasis, and repair, and is involved in the regulation of periodontal cellular activities such as cell proliferation, apoptosis, the secretion of extracellular matrices, the resorption and repair of the root cementum, and remodeling of the alveolar bone proper (31, 33). Although implant therapy has been established and is effective for replacement of a missing tooth, this therapy involves osseointegration into the alveolar bone that does not reconstitute the PDL (44). The regeneration of PDL has been studied previously using cell sheets (17) and stem cells (22), but has not yet been fully successful. It is thought that orthodontic tooth movement, a process involving pathogenic and physiologic responses to extreme forces applied to a tooth through bone remodeling controlled by osteogenesis and osteoclastgenesis (31), is a good assay model for the evaluation of PDL functions. In our present study, the PDL associated with the bioengineered tooth performed in complete cooperation with the oral and maxillofacial regions and bone remodeling successfully occurred following the application of orthodontic mechanical force. These findings indicate that it is possible to restore and re-establish cooperation between the bioengineered tooth and maxillofacial regions and thus regenerate critical dental functions.

The peripheral nervous system plays important roles in the regulation of organ functions and the perception of external stimuli such as pain and mechanical stress (45). During development of the peripheral nervous system, growing axons navigate and establish connections to their developing target organs (46). The recovery of the nervous system, which is associated with the reentry of nerve fibers, is critical for organ replacement (47). Although the functions of several internal organs, including the liver, kidney, and pancreas, are also mediated by specific humoral factors such as hormones and cytokines via blood circulation (45), perceptions of external stimuli are also essential to the functions of several organs, such as the eye, limbs, and teeth (45). The tooth is well recognized as a peripheral target organ for sensory trigeminal nerves, which are required for the function and protection of the teeth (46). It is known also that the perception of mechanical forces during mastication is limited in implant patients (48). Thus, the restoration of nerve functions is also critical for tooth regenerative therapy and future organ replacement therapy (13, 45). In our current study, we demonstrate that several species of nerve fibers, including NF, NPY, CGRP, and galanin-immunoreactive neurons, successfully reentered both the pulp and/or PDL region of the bioengineered tooth. These nerves could thereby transduce the signals from noxious stimulations such as mechanical stress by orthodontic treatment and the exposure of pulp. Previous studies have also revealed that trigeminal nerve fibers navigate and establish their axonal projections into the pulp and PDL during early tooth development in a spatiotemporally controlled manner through expression of regulatory factors such as nerve growth factor, glial cell line-derived neurotrophic factor, and semaphorin 3a (46). Our present results suggest the possibility that the transplantation of regenerated tooth germ can induce trigeminal axon innervation and establishment in an adult jaw through the replication of trigeminal axon pathfinding and nerve fiber patterning during early tooth development (46).

In conclusion, this study provides evidence of a successful replacement of an entire and fully functioning organ in an adult body through the transplantation of bioengineered organ germ, reconstituted by single cell manipulation in vitro. Our study therefore makes a substantial contribution to the development of bioengineering technology for future organ replacement therapy. Further studies on the identification of available adult tissue stem cells for the reconstitution of a bioengineered tooth germ and the regulation of stem cell differentiation into odontogenic cell lineage will help to achieve the realization of tooth regenerative therapy for missing teeth.

Methods

Transplantation. The upper first molars of 5-week-old C57BL/6 (SLC) mice were extracted under deep anesthesia. Mice were maintained for 3 weeks to allow for natural repair of the tooth cavity and oral epithelium. Before transplantation, we confirmed using microCT analysis that the remaining tooth root components and/or the tooth that had developed from them could not be observed in the bony holes (*SI Methods*). Following repair, an incision of approximately 1.5 mm in length was made through the oral mucosa at the extraction site with fine scissors to access the alveolar bone. A fine pin vice (Tamiya) was used to create a bony hole of about 0.5–1.0 mm in diameter in the exposed alveolar bone surface. Just before transplantation, we removed the collagen gel from the bioengineered tooth germ in the in vitro organ culture and marked the top of the dental epithelium with vital staining dye, such as methylene blue, to ensure the correct direction of the explants. The explants were then transplanted into the bony hole according to the dye. The incised oral mucosa was next sutured with 8–0 nylon (8–0 black nylon 4 mm 1/2R, Bear Medic Corp.) and the surgical site was cleaned. The mice containing the transplants were fed a powdered diet (Oriental Yeast) and skim milk until the regenerated tooth had erupted.

ACKNOWLEDGMENTS. We thank Dr. Masaru Okabe (Osaka University) for kindly providing the C57BL/6-TgN (act-EGFP) OsbC14-Y01-FM131 mice. We are also grateful to Dr. Toru Deguchi and Dr. Masahiro Seiryu (Tohoku University) for their analysis of the tooth perceptive potential; Dr. Nobuo Takeshita and Dr. Yuichi Sakai (Tohoku University) for analysis of experimental tooth movement; Dr. Masahiro Saito for critical reading of this manuscript and valuable discussions; and Mr K. Koga (Carl Zeiss) for providing technical support for our microscopic observations. This work was partially supported by Health and Labour Sciences Research Grants from the Ministry of Health, Labour, and Welfare (No. 21040101) to S.K. and T.T., a Grant-in Aid for Scientific Research in Priority Areas (No. 50339131) to T.T., a Grant-in-Aid for Scientific Research (A) and by an "Academic Frontier" Project for Private Universities to T.T. (2003–2007) from Ministry of Education, Culture, Sports and Technology, Japan.

1. Brockes JP, Kumar A (2005) Appendage regeneration in adult vertebrates and implications for regenerative medicine. *Science* 310:1919–1923.

2. Watt FM, Hogan BL (2000) Out of Eden: Stem cells and their niches. *Science* 287:1427–1430.

3. Langer RS, Vacanti JP (1999) Tissue engineering: The challenges ahead. *Sci Am* 280:86–89.
4. Atala A (2005) Tissue engineering, stem cells and cloning: Current concepts and changing trends. *Expert Opin Biol Ther* 5:879–892.
5. Korbling M, Estrov Z (2003) Adult stem cells for tissue repair–a new therapeutic concept? *N Engl J Med* 349:570–582.
6. Chien KR, Moretti A, Laugwitz KL (2004) Development. ES cells to the rescue. *Science* 306:239–240.
7. Nishikawa S, Goldstein RA, Nierras CR (2008) The promise of human induced pluripotent stem cells for research and therapy. *Nat Rev* Mol Cell Biol 9:725–729.
8. Copelan EA (2006) Hematopoietic stem-cell transplantation. *N Engl J Med* 354:1813–1826.
9. Lindvall O, Kokaia Z (2006) Stem cells for the treatment of neurological disorders. *Nature* 441:1094–1096.
10. Segers VF, Lee RT (2008) Stem-cell therapy for cardiac disease. *Nature* 451:937–942.
11. Wang X, et al. (2003) The origin and liver repopulating capacity of murine oval cells. *Proc Natl Acad Sci USA* 100:11881–11888.
12. Griffith LG, Naughton G (2002) Tissue engineering–current challenges and expanding opportunities. *Science* 295:1009–1014.
13. Ikeda E, Tsuji T (2008) Growing bioengineered teeth from single cells: Potential for dental regenerative medicine. *Expert Opin Biol Ther* 8:735–744.
14. Purnell B (2008) New release: The complete guide to organ repair. Introduction. *Science* 322:1489.
15. Lechler RI, Sykes M, Thomson AW, Turka LA (2005) Organ transplantation–how much of the promise has been realized? *Nat Med* 11:605–613.
16. Layer PG, Robitzki A, Rothermel A, Willbold E (2002) Of layers and spheres: The reaggregate approach in tissue engineering. *Trends Neurosci* 25:131–134.
17. Yang J, et al. (2007) Reconstruction of functional tissues with cell sheet engineering. *Biomaterials* 28:5033–5043.
18. Nishida K, et al. (2004) Corneal reconstruction with tissue-engineered cell sheets composed of autologous oral mucosal epithelium. *N Engl J Med* 351:1187–1196.
19. Miyahara Y, et al. (2006) Monolayered mesenchymal stem cells repair scarred myocardium after myocardial infarction. *Nat Med* 12:459–465.
20. Ohashi K, et al. (2007) Engineering functional two- and three-dimensional liver systems in vivo using hepatic tissue sheets. *Nat Med* 13:880–885.
21. Sharpe PT, Young CS (2005) Test-tube teeth. *Sci Am* 293:34–41.
22. Duailibi SE, Duailibi MT, Vacanti JP, Yelick PC (2006) Prospects for tooth regeneration. *Periodontol 2000* 41:177–187.
23. Kuure S, Vuolteenaho R, Vainio S (2000) Kidney morphogenesis: Cellular and molecular regulation. *Mech Dev* 92:31–45.
24. Hogan BL, Yingling JM (1998) Epithelial/mesenchymal interactions and branching morphogenesis of the lung. *Curr Opin Genet Dev* 8:481–486.
25. Pispa J, Thesleff I (2003) Mechanisms of ectodermal organogenesis. *Dev Biol* 262:195–205.
26. Claudinot S, Nicolas M, Oshima H, Rochat A, Barrandon Y (2005) Long-term renewal of hair follicles from clonogenic multipotent stem cells. *Proc Natl Acad Sci USA* 102:14677–14682.
27. Shackleton M, et al. (2006) Generation of a functional mammary gland from a single stem cell. *Nature* 439:84–88.
28. Tucker A, Sharpe P (2004) The cutting-edge of mammalian development; how the embryo makes teeth. *Nat Rev Genet* 5:499–508.
29. Nakao K, et al. (2007) The development of a bioengineered organ germ method. *Nat Methods* 4:227–230.
30. Klingsberg J, Butcher EO (1960) Comparative histology of age changes in oral tissues of rat, hamster, and monkey. *J Dent Res* 39:158–169.
31. Wise GE, King GJ (2008) Mechanisms of tooth eruption and orthodontic tooth movement. *J Dent Res* 87:414–434.
32. Manly RS, Braley LC (1950) Masticatory performance and efficiency. *J Dent Res* 29:448–462.
33. Shimono M, et al. (2003) Regulatory mechanisms of periodontal regeneration. *Microsc Res Tech* 60:491–502.
34. Byers MR, Narhi MV (1999) Dental injury models: Experimental tools for understanding neuroinflammatory interactions and polymodal nociceptor functions. *Crit Rev Oral Biol Med* 10:4–39.
35. Deguchi T, Takeshita N, Balam TA, Fujiyoshi Y, Takano-Yamamoto T (2003) Galanin-immunoreactive nerve fibers in the periodontal ligament during experimental tooth movement. *J Dent Res* 82:677–681.
36. Yen AH, Sharpe PT (2006) Regeneration of teeth using stem cell-based tissue engineering. *Expert Opin Biol Ther* 6:9–16.
37. Ohazama A, Modino SA, Miletich I, Sharpe PT (2004) Stem-cell-based tissue engineering of murine teeth. *J Dent Res* 83:518–522.
38. Song Y, Yan M, Muneoka K, Chen Y (2008) Mouse embryonic diastema region is an ideal site for the development of ectopically transplanted tooth germ. *Dev Dyn* 237:411–416.
39. Duailibi SE, et al. (2008) Bioengineered dental tissues grown in the rat jaw. *J Dent Res* 87:745–750.
40. Zhang W, et al. (2009) Tissue engineered hybrid tooth-bone constructs. *Methods* 47:122–128.
41. Abukawa H, et al. (2009) Reconstructing mandibular defects using autologous tissue-engineered hybrid tooth and bone constructs. *J Oral Maxillofac Surg* 67:335–347.
42. Duailibi MT, et al. (2004) Bioengineered teeth from cultured rat tooth bud cells. *J Dent Res* 83:523–528.
43. Carollo DA, Hoffman RL, Brodie AG (1971) Histology and function of the dental gubernacular cord. *Angle Orthod* 41:300–307.
44. Voruganti K (2008) Clinical periodontology and implant dentistry, 5th edition. *Br Dent J* 205:216.
45. Guyton AC (1967) Textbook of Medical Physiology. *Am J Med Sci* 253:126.
46. Luukko K, Kvinnsland IH, Kettunen P (2005) Tissue interactions in the regulation of axon pathfinding during tooth morphogenesis. *Dev Dyn* 234:482–488.
47. Bengel FM, et al. (2001) Effect of sympathetic reinnervation on cardiac performance after heart transplantation. *N Engl J Med* 345:731–738.
48. Hammerle CH, et al. (1995) Threshold of tactile sensitivity perceived with dental endosseous implants and natural teeth. *Clin Oral Implants Res* 6:83–90.

Regulations of size and shape of the bioengineered tooth by a cell manipulation method

Kazuhisa Nakao[1], Mayumi Murofushi[2], Miho Ogawa[3] & Takashi Tsuji[1,3]

[1] Research Institute for Science and Technology, Tokyo University of Science, Noda, Chiba, 278-8510, JAPAN
[2] Faculty of Industrial Science and Technology, Tokyo University of Science, Noda, Chiba, 278-8510, JAPAN
[3] Organ Technologies Inc., Tokyo, 101-0048, JAPAN

1. ABSTRACT

Regulation of sizes and shapes of tooth are important matters to consider in generating an entirely bioengineered tooth for future tooth replacement therapy. In our current study, we investigated that whether an extent of contact area between epithelial and mesenchymal cell aggregates, which was reconstituted from embryonic day 14.5 molar tooth germ-derived single cells by our cell manipulation method, affect the morphology of the bioengineered tooth. Statistical analysis showed that there were reliable correlations between the contact length of bioengineered tooth germ and the crown widths (R=0.84), and the cusp numbers (R=0.85). These observations indicate that the crown widths and the cusp numbers of bioengineered molar were determined by the contact length between epithelial and mesenchymal cell layers. Our study results will provide important insights into the regulatory mechanisms of sizes and shapes of bioengineered tooth and the application of cell manipulation technology in future tooth replacement therapy.

2. INTRODUCTION

The current approaches being used to develop future regenerative therapies are influenced by our understanding of embryonic development, stem cell biology, and tissue engineering technology [1-4]. One of the more attractive concepts under consideration in regenerative therapy is stem cell transplantation of enriched or purified tissue-derived stem cells [5], or in vitro manipulated embryonic stem (ES) and induced pluripotent stem (iPS) cells [6, 7]. This therapy has the potential to restore the partial loss of organ function by replacing hematopoietic stem cells in hematopoietic malignancies [8], neural stem cells in Parkinson's disease [9], mesenchymal stem cells in myocardial infarction [10], and hepatic stem cells in cases of hepatic insufficiency [11].

The ultimate goal of regenerative therapy is to develop fully functioning bioengineered organs that can replace lost or damaged organs following disease, injury, or aging [4, 12-14]. The feasibility of this concept has essentially been demonstrated by successful organ transplantations for various injuries and diseases [15]. It is expected that bioengineering technology will be developed for the reconstruction of fully functional organs in vitro through the precise arrangement of several different cell species [3, 16-20]. We have recently reported a successful fully functioning tooth replacement in an adult mouse achieved through the transplantation of bioengineered tooth germ into the alveolar bone in the lost tooth region. We propose this technology as a model for future organ replacement therapies. The bioengineered tooth, which was erupted and occluded, had the correct tooth structure, hardness of mineralized tissues for mastication, and response to noxious stimulations such as mechanical stress and pain in cooperation with other oral and maxillofacial tissues [21, 22]. However, the bioengineered tooth was smaller than the other normal teeth, since at present we cannot regulate the crown width, cusp position, and tooth patterning including anterior/posterior and buccal/lingual structures using in vitro cell manipulation techniques.

Here, we showed that the crown widths and the cusp numbers of bioengineered molar could be regulated by cell manipulation method, and were determined by the contact length between epithelial and mesenchymal cell layers but not dependent on the cell number.

3. MATERIALS AND METHODS

3.1 Animals

C57BL/6 mice were purchased from SLC Inc. Mouse care and handling conformed to the NIH guidelines for animal research. All experimental protocols were approved by the Tokyo University of Science Animal Care and Use Committee.

3.2 Reconstitution of bioengineered tooth germ from single cells

Molar tooth germs were dissected from the mandibles of ED14.5 mice. The isolation of tissues and each single cell preparation from epithelium and mesenchyme has been described previously. Dissociated epithelial and mesenchymal cells were precipitated by centrifugation in a siliconized microtube and the supernatant was completely removed. The cell density of the precipitated epithelial and mesenchymal cells after the removal of supernatants reached

978-1-4244-5095-4/09/$26.00 ©2009 IEEE

a concentration of 5 x 10^8 cells/mL as described previously [21]. Bioengineered molar tooth germ was reconstituted using our previously described 3-dimensional cell manipulation method, the 'organ germ method' [21]. We reconstituted various bioengineered tooth germs, which have various contact length between epithelial and mesenchymal cell layers, with uniform thickness using a micro-syringe of 0.330 mm inner diameter (Hamilton). These various bioengineered tooth germs were incubated for 10 min at 37 °C, placed on a cell culture insert (0.4 μm pore diameter; BD), and then further incubated at 37 °C for 5 days in an in vitro organ culture as described previously [21].

3.3 SRC Assay

After 7 dayss incubation, the reconstituted germs of tooth or whisker follicles were transplanted into a subrenal capsule (SRC) for 21 days using 8 week-old male mice as the host, according to the method of Bogden and co-workers [23].

3.4 Microcomputed Tomography (MicroCT)

The heads of mice implanted with bioengineered tooth germ and control mice were fixed in the centric occlusal position and radiographic imaging was then performed by x-ray using an inspeXio SMX-90CT device (Shimadzu) with exposure at 90 kV and 0.1 mA, and with a source-to-sample distance of 34 mm. Microcomputed tomography was performed using Imaris (Carl Zeiss).

3.5 Tissue Preparation

The tissues were removed and immersed in 4% paraformaldehyde in PBS(-). After fixation, the tissues were decalcified in 4.5% EDTA (pH 7.4) for 1-10 days at 4°C. The sections were observed using an Axio Imager A1 (Carl Zeiss, Jena, Germany) with an AxioCAM MRc5 (Zeiss) and processed with AxioVision software (Zeiss).

4. RESULTS AND DISCUSSION

We first investigated that whether an extent of contact area between epithelial and mesenchymal cell aggregates, which was reconstituted from embryonic day 14.5 molar tooth germ-derived single cells by our cell manipulation method, affect the morphology of the bioengineered tooth. We reconstituted various bioengineered tooth germs, which have various contact length between epithelial and mesenchymal cell layers, with uniform thickness using a micro-syringe of 0.330 mm inner diameter. After a day of organ culture, we categorized into three-types of the bioengineered tooth germ by the contact length: group I, up to 450 μm; group II, 450-900 μm; and group III, 900-1500 μm. The bioengineered molar tooth germ in group I to III had developed at the early bell stage of a natural tooth germ after 5-7 days growth and were with a mean width of each 366 ± 103 μm, 584 ± 103 μm and 934 ± 239 μm, respectively (Fig. 1a). Statistical analysis revealed that there were significant correlations between the contact length and the mean width of the bioengineered molar tooth germs (R=0.89) (Fig. 1b).

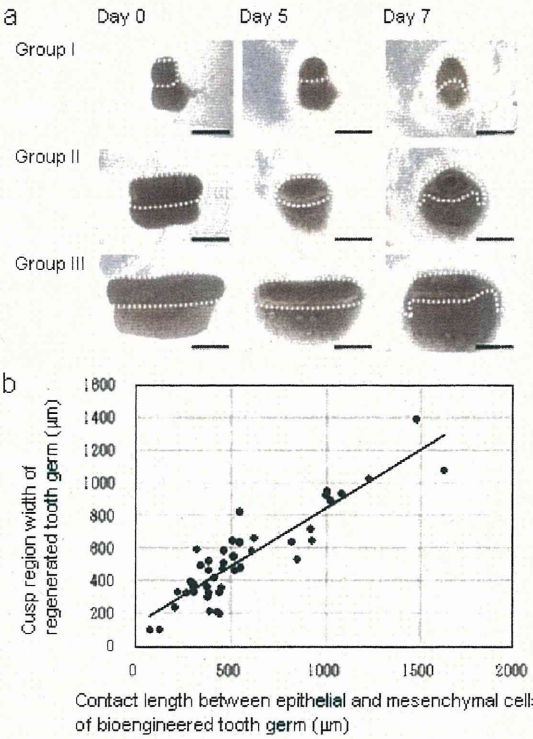

F

Regulation of the width of bioengineered tooth germ by cell manipulation method. (a) Phase contrast image of three-types of the bioengineered tooth germ on day 0, day 5 and day 7 of an organ culture. (Scale bar, 500 μm.) (b) Scatter diagram of correlational analysis between the contact length and the width of the bioengineered tooth germ.

After 21 days transplantation in subrenal capsule, the bioengineered molars developed from the bioengineered germs in group I to III were with a mean crown widths of each 497 ± 118 μm, 727 ± 271 μm and 1073 ± 186 μm, respectively (Fig. 2a). The bioengineered tooth formed a correct structure comprising enamel, ameloblast, dentin, odontoblast, dental pulp, alveolar bone, and blood vessels (Fig. 2a). Moreover, the cusp numbers of those teeth derived from the bioengineered germs in group I to III were 2.9 ± 0.8, 4.7 ± 3.1 and 11 ± 2.6, respectively (Fig. 2a). Statistical analysis showed that there were reliable correlations between the contact length of bioengineered tooth germ and the crown widths (R=0.84) (Fig. 2b), and the cusp numbers (R=0.85) (Fig. 2c).

Finally, we examined that whether the cell number of epithelial and mesenchymal cells influences the morphology of the bioengineered tooth. We formed the cell aggregates with different thickness by use of micro-syringe of 0.203

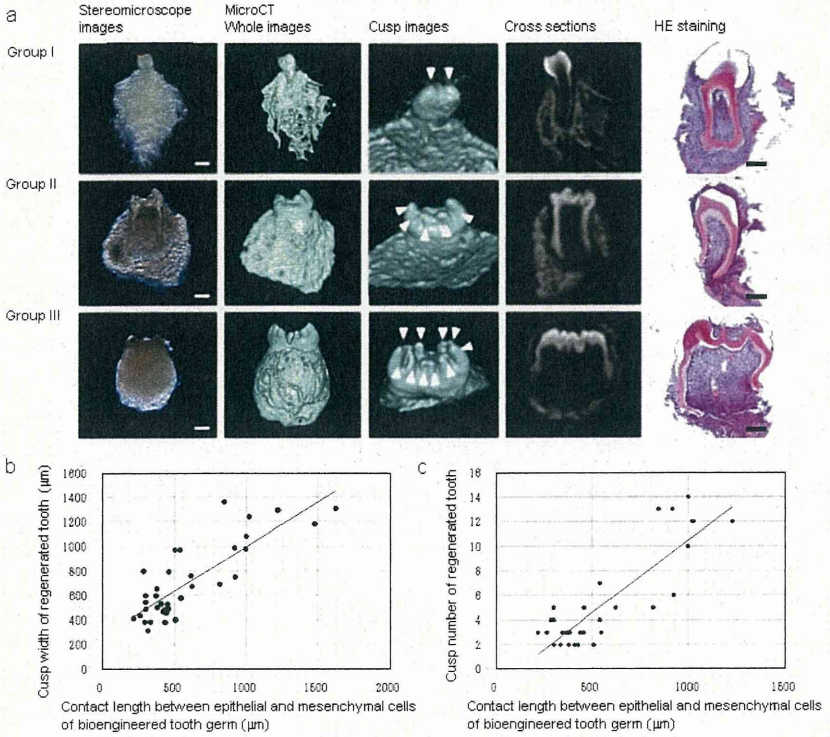

Fig. 2
Regulation of the crown width and cusp number of bioengineered tooth by cell manipulation method. (a) Morphological and histological analysis of three-types of the bioengineered tooth after 21 days transplantation. Stereomicroscope images (first columns from the left), whole images of MicroCT (second columns), Cusp images (third columns), cross sections (fourth columns) are shown. Arrow head, cusp. (Scale bar, 200 μm). (b) Scatter diagram of correlational analysis between the contact length and the crown width of the bioengineered tooth. (c) Scatter diagram of correlational analysis between the contact length and the cusp number of the bioengineered tooth.

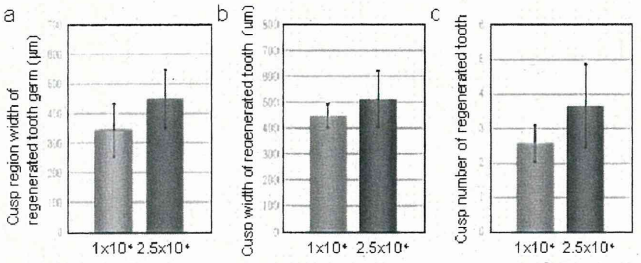

Fig. 3
Morphological differences of the bioengineered tooth by regulating cell number. Cusp region width of the bioengineered tooth germ on day 7 organ culture (a), crown width (b) and cusp number (c) of the bioengineered tooth after 21 days transplantation are shown.

mm or 0.330 mm inner diameter while limiting the contact length to 300-500 μm. However, there were no differences in the crown widths and cusp numbers of the bioengineered molar between $1x10^4$ cells per aggregate and $2.5x10^4$ cells per aggregate ($p>0.06$) (Fig. 3a, b and c). These results indicated that the crown widths and the cusp numbers of bioengineered molar were determined by the contact length between epithelial and mesenchymal cell layers but not dependent on the cell number.

In conclusion, this study provides an important insight into the regulatory mechanisms of sizes and shapes of bioengineered tooth and the application of cell manipulation technology in future tooth replacement therapy. Further studies on the identification of available adult tissue stem cells for the reconstitution of a bioengineered tooth germ and the regulation of stem cell differentiation into odontogenic cell lineage will help to achieve the realization of tooth regenerative therapy for missing teeth.

5. ACKNOWLEDGEMENT

This work was partially supported by a Grant-in Aid for Scientific Research in Priority Areas (No. 50339131) to T.T., a Grant-in-Aid for Scientific Research (A) and by an ''Academic Frontier'' Project for Private Universities to T.T. (2003–2007) from Ministry of Education, Culture, Sports and Technology, Japan.

6. REFERENCES

1. Brockes JP, Kumar A. *Science* **310**, 1919–1923 (2005).
2. Watt FM, Hogan BL. *Science* **287**, 1427–1430 (2000).
3. Langer RS, Vacanti JP. *SciAm***280**, 86–89 (1999).
4. Atala A. *Expert Opin Biol Ther* **5**, 879–892 (2005) .
5. Korbling M, Estrov Z. *N Engl J Med* **349**, 570–582 (2003).
6. Chien KR, Moretti A, Laugwitz KL. *Science* **306**, 239–240 (2004).
7. Nishikawa S, Goldstein RA, Nierras CR. *Nat Rev* Mol Cell Biol **9**, 725–729 (2008).
8. Copelan EA. *N Engl J Med* **354**, 1813–1826 (2006).
9. Lindvall O, Kokaia Z. *Nature* **441**, 1094–1096 (2006).

10. Segers VF, Lee RT. *Nature* **451**, 937–942 (2008).
11. Wang X, et al. *Proc Natl Acad Sci USA* **100**, 11881–11888 (2003).
12. Griffith LG, Naughton G. *Science* **295**, 1009–1014 (2002).
13. Ikeda E, Tsuji T. *Expert Opin Biol Ther* **8**, 735–744 (2008).
14. Purnell B. *Science* **322**, 1489 (2008).
15. Lechler RI, Sykes M, Thomson AW, Turka LA. *Nat Med* **11**, 605–613 (2005).
16. Layer PG, Robitzki A, Rothermel A, Willbold E. *Trends Neurosci* **25**, 131–134 (2002).
17. Yang J, et al. *Biomaterials* **28**, 5033–5043 (2007).
18. Nishida K, et al. *N Engl J Med* **351**, 1187–1196 (2004).
19. Miyahara Y, et al. *Nat Med* **12**, 459–465 (2006).
20. Ohashi K, et al. *Nat Med* **13**, 880–885 (2007).
21. Nakao K, et al. *Nat Methods* **4**, 227–230 (2007).
22. Ikeda E, Morita R, et al. *Proc Natl Acad Sci USA,* Epub ahead of print (2009).

Biochemical and Biophysical Research Communications 405 (2011) 455–461

Contents lists available at ScienceDirect

Biochemical and Biophysical Research Communications

journal homepage: www.elsevier.com/locate/ybbrc

The regulation of tooth morphogenesis is associated with epithelial cell proliferation and the expression of *Sonic hedgehog* through epithelial–mesenchymal interactions

Kentaro Ishida [a], Mayumi Murofushi [a], Kazuhisa Nakao [b], Ritsuko Morita [b], Miho Ogawa [b,c], Takashi Tsuji [a,b,c,*]

[a] Faculty of Industrial Science and Technology, Tokyo University of Science, Chiba 278-8510, Japan
[b] Research Institute for Science and Technology, Tokyo University of Science, Chiba 278-8510, Japan
[c] Organ Technologies Inc., Tokyo 101-0048, Japan

ARTICLE INFO

Article history:
Received 25 December 2010
Available online 19 January 2011

Keywords:
Tooth morphogenesis
Organ germ method
Sonic hedgehog
Epithelial–mesenchymal interaction

ABSTRACT

Ectodermal organs, such as the tooth, salivary gland, hair, and mammary gland, develop through reciprocal epithelial–mesenchymal interactions. Tooth morphologies are defined by the crown width and tooth length (macro-morphologies), and by the number and locations of the cusp and roots (micro-morphologies). In our current study, we report that the crown width of a bioengineered molar tooth, which was reconstructed using dissociated epithelial and mesenchymal cells via an organ germ method, can be regulated by the contact area between epithelial and mesenchymal cell layers. We further show that this is associated with cell proliferation and *Sonic hedgehog* (*Shh*) expression in the inner enamel epithelium after the germ stage has formed a secondary enamel knot. We also demonstrate that the cusp number is significantly correlated with the crown width of the bioengineered tooth. These findings suggest that the tooth micro-morphology, i.e. the cusp formation, is regulated after the tooth width, or macro-morphology, is determined. These findings also suggest that the spatiotemporal patterning of cell proliferation and the *Shh* expression areas in the epithelium regulate the crown width and cusp formation of the developing tooth.

1. Introduction

All organs arise from their respective germs through reciprocal interactions between the epithelium and mesenchyme during organogenesis in the developing embryo [1–4]. Organs develop according to predetermined programs, which include the regulation of their location, cell number and morphology. The induction of organ development at the appropriate future location requires both regional and genetic specificity [5]. It is well known in this regard that many cytokines, such as the fibroblast growth factor (FGF), hedgehog, Wnt, and transforming growth factor (TGF)/bone morphogenetic protein (BMP) families, play essential roles in epithelial and mesenchymal interactions during organogenesis [1,2].

Ectodermal organs, such as the tooth, salivary gland, hair, and mammary gland, also develop through reciprocal epithelial and mesenchymal interactions [1,2]. The number and morphology of the teeth in the tooth forming field, which are specified by the expression of homeobox genes in the underlying neural crest-derived mesenchyme in the embryonic jaw, have previously been determined during developmental process [3]. Tooth development begins with epithelium thickening and innervation of the underling mesenchyme [1,2]. At the dental placode stage, the dental epithelium induces the condensation of the surrounding mesenchymal cells through the expression of signaling molecule genes such as *Shh*, *Fgf8*, *Bmp4* and *Wnt10b*, which can induce the expression of a large number of transcription factors such as *Msx1*, *Pax9* and *Gli* in the mesenchyme [2]. These interactions between these signaling molecules and transcription factors induce the formation of an enamel knot, which acts as a signaling center to coordinate tooth germ development [2]. *Shh* plays a particularly important role in tooth germ induction and formation, including the primary enamel knot formation, and thereafter functions in the growth and differentiation of epithelial cells into the ameloblast [6].

Following tooth germ formation, the epithelial and mesenchymal cells in the tooth germ differentiate into tooth-tissue forming cells and secrete hard tissues such as enamel dentin, cementum, and alveolar bone [7]. The tooth types that result, such as incisors (monocuspid) and molars (multicuspid), are thought to be

* Corresponding author at: Department of Biological Science and Technology, Faculty of Industrial Science and Technology, Tokyo University of Science, Noda, Chiba 278-8510, Japan. Fax: +81 4 7122 1499.
E-mail addresses: t-tsuji@rs.noda.tus.ac.jp, t-tsuji@nifty.com (T. Tsuji).

0006-291X/$ - see front matter © 2011 Elsevier Inc. All rights reserved.
doi:10.1016/j.bbrc.2011.01.052

regulated by regional gene expression which controls the tooth-forming region at the mesenchyme during embryonic development [3]. It has also been reported that the tooth type and morphology is determined by the balance of endogenous inhibitors and mesenchymal activator [8] and by regulatory mechanisms that operate in the tooth forming field [9]. Tooth morphology is defined by both the crown size and tooth length at the macro-morphology, and by the number and position of the cusp and roots at the micro-morphology [10]. Although the crown size, as a determinant of macro-patterning during tooth morphogenesis, is based on the reaction-diffusion model [10], the underlying molecular and cellular mechanisms, such as cell growth and cell movement, have remained unexplored. The regulation of the cusp number and position, which underlies the micro-patterning of the tooth, is thought to be closely involved in the formation of the secondary enamel knot. This is regulated spatiotemporally by the reciprocal activation and inhibition of cell proliferation in the epithelium and mesenchyme via the reaction-diffusion mechanism, and determines the cusp pattern formation through cell growth and movement [11,12]. However, it remains to be undetermined how the regulation of cell proliferation and the underlying molecular mechanisms are involved in crown size determination through epithelial–mesenchymal interactions.

In our current study, we analyzed the mechanisms that determine the crown width and cusp number of a bioengineered tooth via the regulation of the contact area between the epithelial and mesenchymal cell layers. We provide evidence to suggest that the spatiotemporal regulation of epithelial cell proliferation and *Shh* expression in the tooth germ-epithelium is involved in determining the crown and cusp morphologies during tooth development.

2. Materials and methods

2.1. Animals

C57BL/6 mice were purchased from SLC Inc., (Shizuoka, Japan). B6.Cg-*Shh*$^{tm1(EGFP/cre)Cjt}$/J mice were obtained from The Jackson Laboratory (Bar Harbor, ME). All mouse care and handling complied with the NIH guidelines for animal research and all experimental protocols involving animals were approved by the Tokyo University of Science Animal Care and Use Committee.

2.2. Reconstitution of a bioengineered tooth germ from single cells

Molar tooth germs were dissected from the mandibles of ED14.5 mice in order to reconstitute a bioengineered tooth germ by a three-dimensional cell manipulation method, the previously described organ germ method [13]. To regulate the contact length between the epithelial and mesenchymal cell layers, the epithelial and mesenchymal columnar cell layers were arranged contiguously using a micro-syringe with a 0.330 μm inner diameter to inject both cell types into a 30 μm gel drop of Cellmatrix type I-A (Nitta gelatin, Osaka, Japan). The contact length between epithelial and mesenchymal cell layers was then measured using Axioobserver (Carl Zeiss, Jena, Germany) with an AxioCAM MRc5 (Carl Zeiss) microscope and Axiovision software (Carl Zeiss). The resulting bioengineered tooth germs were incubated at 37 °C for 2–7 days as described previously [13].

2.3. Microcomputed tomography (Micro-CT) measurements

Radiographic imaging was performed using X-rays and a Micro-CT device (R_mCT, Rigaku) with exposures set at 90 kV and 150 mA. Micro CT images were captured using i-view R (Morita) and Imaris (Carl Zeiss).

2.4. Histochemical and immunohistochemical analysis

Histochemical tissue analyses were performed as described previously [13]. Briefly, tissue sections (10 μm) were stained with hematoxylin and eosin and observed using Axioimager A1 (Carl Zeiss) with an AxioCAM MRc5 (Carl Zeiss) microscope. Tissues were prepared for immunohistochemistry as described previously [14]. For fluorescent immunohistochemistry, the tissue sections (10 μm) were incubated with an anti-Ki67 primary antibody (1:100; Abcam, Cambridge, MA) and Hoechst33342 (1:500; Invitrogen, Carlsbad, CA) for 2 h at room temperature. Immunoreactivity was detected using an Alexa Fluor® 594-conjugated Goat Anti-rabbit IgG secondary antibody (1:500, Invitrogen). Fluorescence microscopy images were captured under a confocal microscope (LSM 510; Carl Zeiss) and processed with AxioVision software (Carl Zeiss).

2.5. In situ hybridization

In situ hybridizations were performed using 10 μm frozen sections as described previously [13]. Digoxygenin-labeled probes for specific transcripts were prepared by PCR with primers designed using published sequences (*Shh*; GenBank ID: NM_009170, *Fgf4*; GenBank ID: NM_010202, *Fgf3*; GenBank ID: NM_008007).

2.6. Statistical analysis

Statistically-significant differences were determined by the unpaired student's *t*-test. The analysis was performed using the Common Gateway Interface Program (twk, Saint John's University).

3. Results

3.1. The crown width of a bioengineered tooth correlates with the length of the contact area between the epithelial and mesenchymal cell layers

We first investigated whether the contact area between the epithelial and mesenchymal cell layers affect the eventual morphology, such as the crown width and cusp number, of a bioengineered tooth germ reconstituted from ED14.5 molar tooth germ-derived single cells using the organ germ method [13]. The bioengineered tooth germs, which were prepared using various contact lengths between the epithelial and mesenchymal cell layers, were reconstructed with a micro-syringe of a 0.330 μm inner diameter (Fig. 1A). After one day of *in vitro* organ culture, we classified the bioengineered tooth germs into three-groups by measuring the contact length using a side-view as follows: short-contact length (short), up to 450 μm; middle-contact length (middle), 450–900 μm, and long-contact length (long), 900–1500 μm. The mean widths were also calculated as follows: short, 366 ± 103 μm; middle, 584 ± 103 μm; and long, 934 ± 239 μm. All of the bioengineered tooth germs reached the early bell developmental stage at the same time as a natural tooth germ following 3–5 days in culture (Fig. 1B). To examine the correlation between the contact length and the tooth crown width of the bioengineered teeth, the germs were transplanted into a subrenal capsule. At 21 days post-transplantation, the entire bioengineered tooth germ developed into a tooth unit with the correct structure comprising enamel, ameloblast, dentin, odontoblast, dental pulp, alveolar bone, and blood vessels (Fig. 1C). Typical images of these teeth classified into the three-groups above are shown in Fig. 1C. The mean crown widths of the bioengineered molars that developed from the short, middle and long germ groups were 497 ± 118 μm, 727 ± 271 μm, and 1073 ± 186 μm, respectively. All of the crown widths of the samples following subrenal capsule

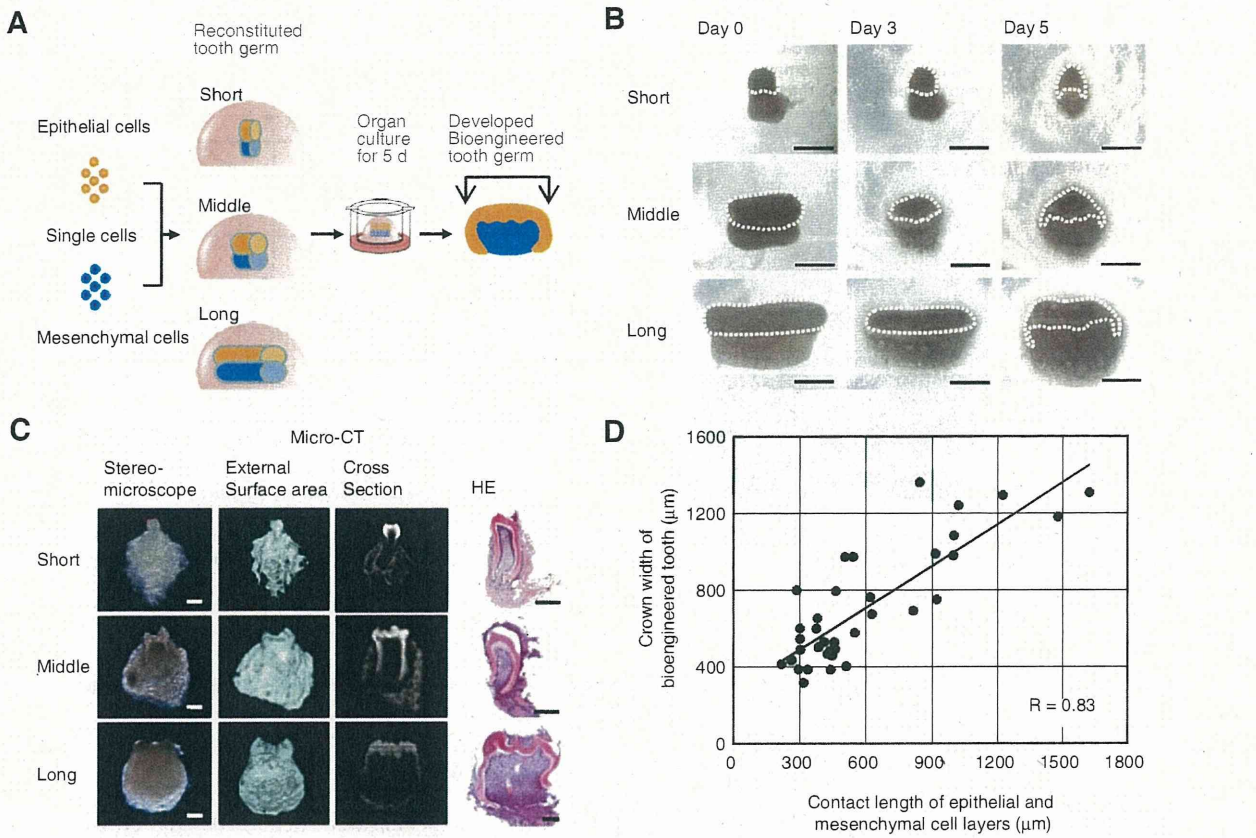

Fig. 1. The crown width of a bioengineered tooth correlates with the length of the contact area between the epithelial and mesenchymal cell layers. (A) Schematic representation of the bioengineering technology used for the generation of bioengineered tooth germ of various contact lengths between epithelial and mesenchymal cell layers. (B) Phase contrast images of the three contact area groups (upper, short; middle, middle; lower, long) of the bioengineered tooth germs on days 0, 3, and 5 of organ cultures. Scale bars, 200 μm. (C) Representative images of the three contact area bioengineered tooth groups (upper, short; middle, middle; lower, long) developed in a subrenal capsule environment for 21 days. Stereomicroscope (first columns from the left), external images (second columns) and cross sections (third columns) of Micro CT and hematoxylin and eosin staining (fourth columns) are shown. Scale bars, 200 μm. (D) Scatter diagram showing correlations between the contact lengths between epithelial and mesenchymal cells and the crown widths of the resulting bioengineered tooth ($R = 0.83$).

transplantation were then plotted and statistical analysis indicated a reliable correlation between the contact lengths of the bioengineered tooth germs and the crown widths of the resulting teeth ($R = 0.83$; Fig. 1D). These results indicate that the crown width is controlled by the contact area between the epithelial and mesenchymal cell layers.

3.2. The cusp number of the bioengineered teeth correlates with their crown width

We next examined whether the crown width affects the determination of the cusp number in the bioengineered teeth. At 21 days post-transplantation into the subrenal capsule, the cusp numbers of the bioengineered teeth were analyzed by Micro-CT (Fig. 2A). Statistical analysis indicated a reliable correlation between the contact length of the bioengineered tooth germs and the resulting cusp numbers of the bioengineered teeth ($R = 0.87$; Fig. 2B). These observations suggest that the eventual cusp number is indeed dependent on the crown width.

3.3. The Shh expression area correlates with the crown width in developing tooth germ

Sonic hedgehog (*Shh*) and *fibroblast growth factor 4* (*Fgf4*) play important roles in the early development of tooth germ [1,2]. We next investigated the expression patterns of these factors during the early developmental stages of both natural molar and bioengineered tooth germ. During natural tooth germ development, *Shh* and *Fgf4* mRNA-positive cells can be observed in the enamel knot, which is the epithelial signaling center, at ED13.5 and ED14.5 (Fig. 3A). Interestingly, the *Shh* expression area was found to extend from the enamel knot to the inner enamel epithelium, in accordance with the progression of crown development, but was restricted in the inner enamel epithelium at the prospective occlusal region, but not at the lateral region, at ED15.5 and ED16.5 (Fig. 3A). In contrast, *Fgf4* mRNA-positive cells were found to be restricted locally throughout the early period of crown development and these transcripts were detectable in the enamel knot at ED13.5–ED15.5 and in the secondary enamel knot at ED16.5 (Fig. 3A). In the case of the bioengineered molar germ, the expression patterns of *Shh* and *Fgf4* mRNAs were identical to those of the natural tooth germ (Fig. 3A). *Shh* expression was restricted to the enamel knot after 2 days and to the inner enamel epithelium at the prospective occlusal region after 3–7 days of organ culture (Fig. 3A). *Fgf4* expression was detected in the enamel knot after 3–5 days and in the secondary enamel knot after 7 days organ culture (Fig. 3A). The expression of *Fibroblast growth factor 3* (*Fgf3*), which is also thought to be an important mesenchymal signaling molecule, was detectable in the dental papillae adjacent to the *Shh*-expressing inner enamel epithelium throughout the early period of development in both natural and bioengineered tooth germ (Fig. 3B). Hence, although the development of bioengineered tooth

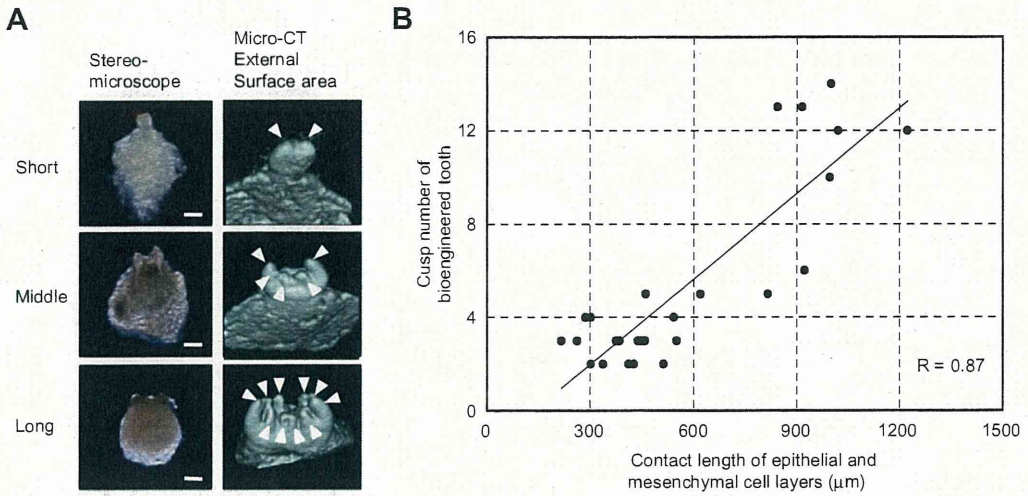

Fig. 2. The cusp number of the bioengineered tooth correlates with its crown width. (A) Stereomicroscope (left) and Micro CT (right) images of bioengineered teeth from the three contact area groups. Cusps are indicated by arrowheads. Scale bars, 200 μm. (B) Scatter diagram analysis of the correlation between the crown width and cusp number in bioengineered teeth ($R = 0.87$).

germ is delayed compared with natural germ, the molecular mechanisms regulating early tooth germ development are similar for both bioengineered and natural tooth germ.

We further examined the correlation between the width of *Shh*-expressing area in the inner enamel epithelium at the prospective occlusal region and the crown width of the bioengineered tooth germ. We generated bioengineered molar tooth germs from the three contact area groups over three days in organ culture. The *Shh*-expression area was found to be extended from the enamel knot to the inner enamel epithelium at the prospective occlusal region, but not at the lateral region, over the culture period, and the width of this area was observed to be equivalent to the width of prospective crown of bioengineered tooth germ (Fig. 3C). These results suggest that the *Shh*-expression pattern in the inner enamel epithelium is closely associated with the mechanisms that regulate crown width.

3.4. The spatiotemporal epithelial cell growth that correlates with the Shh expression pattern is involved in the regulation of crown size

We finally investigated whether the spatiotemporal *Shh* expression pattern shown in Fig. 3 is involved in the patterning of epithelial cell proliferation during tooth germ development. We therefore analyzed *Shh* expression using a transgenic mouse expressing green fluorescent protein (GFP) at the *Shh* locus (*ShhGFP* mice). We measured cell proliferation by immunohistochemical analysis of Ki67 in natural and bioengineered tooth germs. In a natural ED14.5 molar tooth germ, *Shh* expression in an *in vitro* organ culture shows the same expression pattern as that detected by *in situ* hybridization *in vivo* (Figs. 3A and 4A). Cell proliferation in natural tooth germ detected by Ki67 was evident at the cervical loop after one day and the lateral region of the epithelium after 2–4 days, in which *Shh* expression was not found (Fig. 4A). The bioengineered molar tooth germ showed expression of *Shh* at the first enamel knot on day 3 and in the inner enamel epithelium in the prospective occlusal region at day 6 in an organ culture. Cell proliferation of the bioengineered germ was also observed in the *Shh* expression-negative regions at the cervical loop and inner enamel epithelium in the lateral region after 6 days of organ culture (Fig. 4B). These results suggest that the crown width is determined by the spatiotemporal area patterning of the *Shh* expression-positive and cell proliferation-negative regions of the inner enamel epithelium during the early bell stage.

4. Discussion

We demonstrate herein that the crown width of a bioengineered tooth is regulated by the contact area between the epithelial and mesenchymal cell layers and associates with cell proliferation and *Shh* expression in the inner enamel epithelium. We also demonstrate that the cusp number is significantly correlated with the crown width of the bioengineered tooth. These findings also suggest that the spatiotemporal patterning of the cell proliferation and *Shh* expression areas in epithelium regulates the crown width and cusp formation of the tooth.

At the initiation phase of tooth germ development, the tooth-forming field and the basic pattern of dentition (molar and incisor) are regulated by the coordination of gene expression patterning [3]. Rostral–caudal patterning determines the tooth-forming field through the expression patterns of *Lhx6/7* and *Gsc* [3]. On the other hand, proximal-distal patterning determines the molar and incisor fields through the formation of gene expression patterning between *Bmp4* and *Fgf8* in the epithelium, and these gene products then induce *Msx1/2*, *Barx1* and *Dlx2* in the mesenchyme [3]. It is thought that the number of teeth, the sizes of which are also determined by the size of the tooth germ, is proportional to the size of the tooth-forming field [3]. A previous study has indicated that the final crown size is memorized in the dental mesenchyme and regulated by the reaction-diffusion model [10]. In our current study, we provide evidence that the crown width is determined by the contact area between the epithelial and mesenchymal cell layers. We also demonstrate that the *Shh*-expressing region in the dental epithelium of not only natural but also the bioengineered tooth germ gradually enlarges to the final size of the crown width, and that cell proliferation does not occur in the *Shh*-expression region. These findings indicate that cell proliferation is essential for the determination of the crown width in the inner enamel epithelium at the prospective occlusal region, in which the cells express *Shh*, and also for tooth root formation in the cervical loop region. It has been reported previously that *Shh* regulates epithelial proliferation, cell survival, and tooth size [15]. Our present results suggest the possibility that the spatiotemporal regulation of

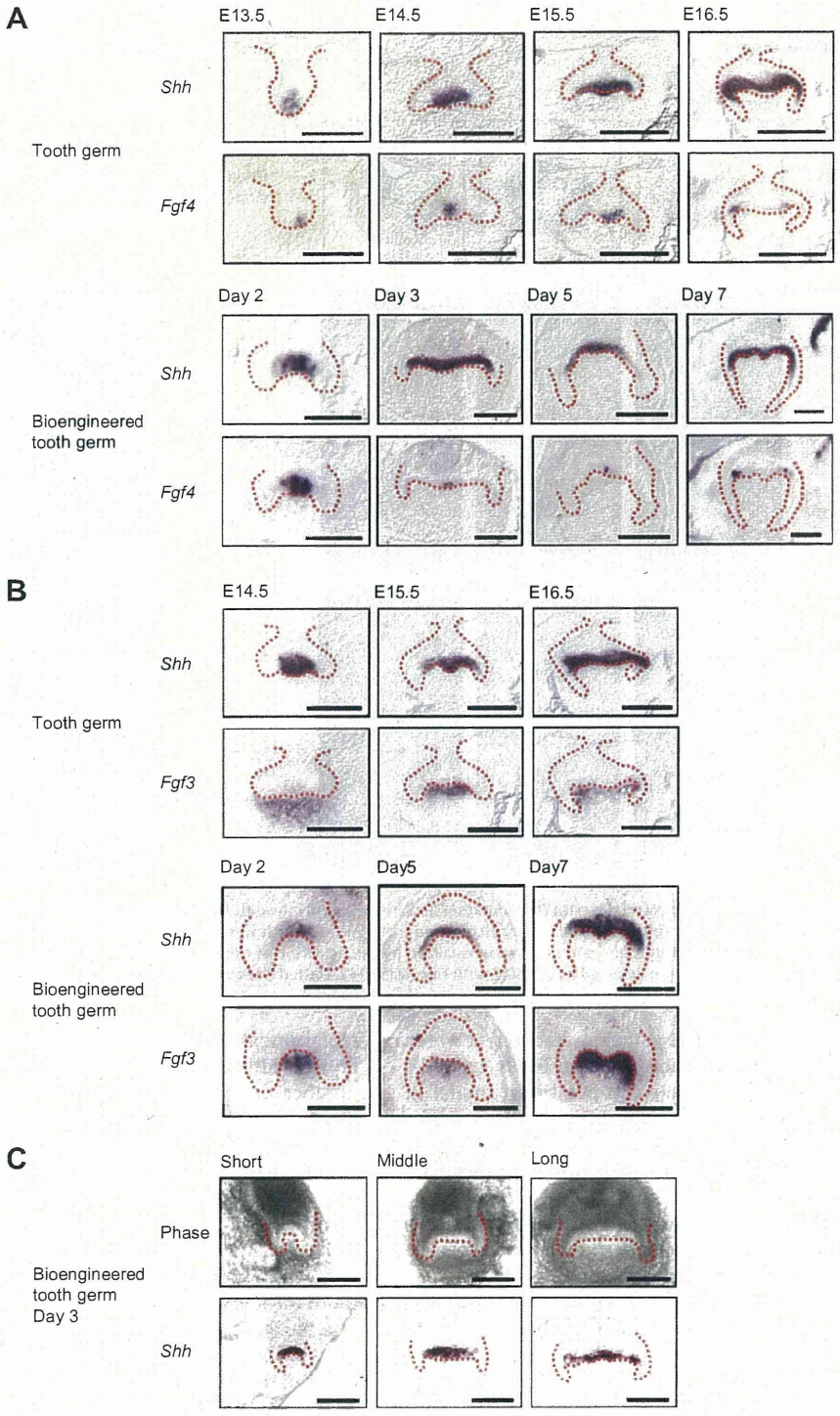

Fig. 3. The width of the *Shh* expression area correlates with the crown width in the developing tooth germ. (A) *In situ* hybridization analyses of the *Shh* and *Fgf4* expression profiles in natural tooth germ at ED13.5–ED16.5 and in bioengineered tooth germ after 2, 3, 5, and 7 days of organ culture. (B) Expression patterns of *Shh* and *Fgf3* in natural tooth germ at ED14.5–ED16.5 and bioengineered tooth germ after 2, 5, and 7 days of organ culture. (C) Phase contrast images and expression analysis of *Shh* mRNA in the three contact area groups of bioengineered tooth germ after three days of cultivation. Dotted lines indicate the boundaries between the epithelium and mesenchyme. The area inside the line is the epithelium. Scale bars, 200 μm.

epithelial cell proliferation and *Shh* expression are closely involved in the determination of tooth macro-morphology and represent the molecular basis of tooth size determination.

A reaction-diffusion model has been predicted and analyzed in the patterning of micro-structures such as digits in limbs, feathers in skin, and cusps in tooth [11,16,17]. Previous studies have suggested that the number of digits in the mouse limb is regulated by not only the width of the mesoderm but also the length of the *Fgf4*-expressing apical ectodermal ridge, which is the signaling center in limb development [18]. In tooth development, it is thought that the cusp patterning is regulated by the secondary enamel knots, which is one of the signaling centers for cusp

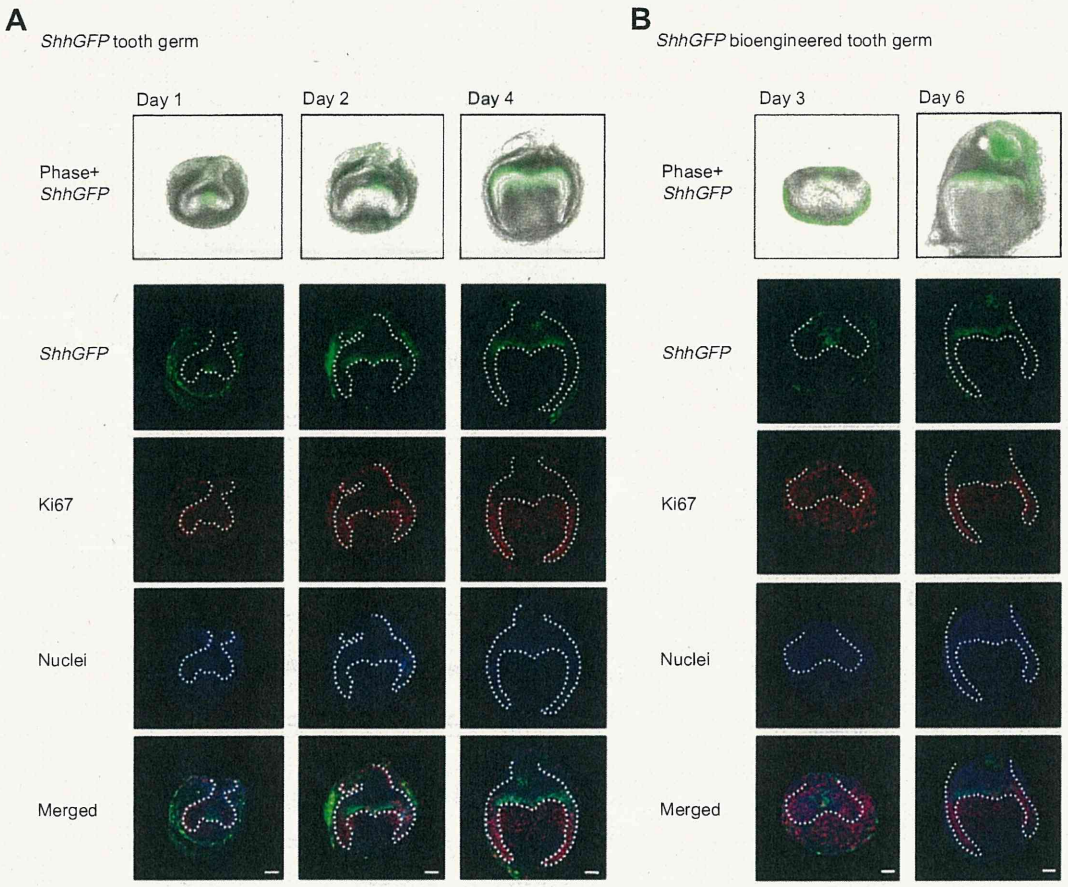

Fig. 4. The spatiotemporal epithelial cell growth correlates with the *Shh* expression area and is involved the regulation of crown size. (A) Molar germs isolated from an *ShhGFP* mouse at ED14.5 after 1, 2, and 4 days of organ culture. (B) *ShhGFP* bioengineered tooth germs, which were generated from the molar germs of an *ShhGFP* mouse at ED14.5, were examined after 3 and 6 days of organ culture. *Shh* expression was visualized by the detection of GFP signals. Cell proliferation was immunohistochemically analyzed using a specific antibody against Ki67. Nuclei were detected by staining with Hoechst33342. Dotted lines indicate the boundaries between the epithelium and mesenchyme. Scale bars, 100 μm.

formation, and might be regulated by the interaction between FGF4, as an activator of cusp formation, and the BMPs and SHH as inhibitors [19]. Based on an earlier computational model of mammalian tooth development, there may be a simple basis for the variations in cusp patterning which can be explained by changes in single model parameters [12,20]. Although there are several reports regarding the determination of tooth size and cusp number, the mechanisms suggested in these studies remain controversial. It was previously reported that each tooth and cusp size is determined by each mesenchyme and epithelium, respectively, through species-specific biological programs [10]. It has also been suggested that the number of developing cusps of a tooth reconstituted from dental epithelium and dissociated mesenchymal cells was enlarged by increasing the mesenchymal cell number [21]. Furthermore, it has been suggested that the number of cusps, a micro-patterning event, is regulated by waves which are determined by the tooth size i.e. macro-patterning, in a reaction-diffusion model [10]. Our present findings indicate that the cusp number in a bioengineered tooth is significantly correlated with the crown width, which is regulated by the contact area between the epithelial and mesenchymal cell layers. These findings suggest that the micro-patterning of cusp formation is regulated after tooth size determination (i.e. macro-patterning) through the number and length of waves in a reaction-diffusion model.

Currently, it is anticipated that organ replacement therapy will represent the next generation of regenerative medical technology and successfully replace lost or damaged organs [22]. For such replacement tissues to function correctly, it will be necessary to reproduce the organ mass through the generation of a sufficient number of functional cells, and faithful replication of both the macro- and micro-morphologies [23]. As a concept for organ regeneration, an approach to developing a functional bioengineered organ from a bioengineered organ germ by reproducing the developmental process during organogenesis has now been investigated [4,24]. We have also previously reported from our laboratory that a bioengineered tooth germ reconstituted using an organ germ method can regenerate a fully functional bioengineered tooth through transplantation [14]. It is thought that the regulation of a bioengineered tooth morphology, such as the crown size and the number and location of the cusps, is important for occlusion to properly occur [11], which is an essential issue for future tooth regenerative therapy [4,24]. Previously, it has been reported that the morphology of a bioengineered tooth can be regulated by culturing tooth germ cells onto a tooth-shaped biodegradable scaffold [24]. In our present study, our cell manipulation technique to regulate the contact area between epithelial and mesenchymal cell layers will make a substantial contribution to the future clinical application of bioengineered teeth.

Our present data suggest that the spatiotemporal patterning of cell proliferation and *Shh* expression areas in the epithelium regulates the crown width and cusp formation of the tooth. Further studies of the molecular mechanisms underlying cell proliferation, differentiation and cell movement will contribute further to our understanding of tooth organogenesis. The development of future

technologies to more precisely regulate the morphology of bioengineered teeth will be required to realize tooth regenerative therapy.

Acknowledgments

This work was partially supported by Health and Labour Sciences Research Grants from the Ministry of Health, Labour, and Welfare (No. 21040101), a Grant-in-Aid for Scientific Research in Priority Areas (No. 50339131), a Grant-in-Aid for Scientific Research (A) from Ministry of Education, Culture, Sports and Technology, Japan (all to T.T.).

References

[1] J. Pispa, I. Thesleff, Mechanisms of ectodermal organogenesis, Dev. Biol. 262 (2003) 195–205.
[2] I. Thesleff, Epithelial–mesenchymal signalling regulating tooth morphogenesis, J. Cell Sci. 116 (2003) 1647–1648.
[3] A. Tucker, P. Sharpe, The cutting-edge of mammalian development; how the embryo makes teeth, Nat. Rev. Genet. 5 (2004) 499–508.
[4] P.T. Sharpe, C.S. Young, Test-tube teeth, Sci. Am. 293 (2005) 34–41.
[5] S.F. Gilbert, Developmental Biology, ninth ed., Sinauer, Massachusetts, 2010.
[6] A. Gritli-Linde, M. Bei, R. Maas, X.M. Zhang, A. Linde, A.P.. McMahon, Shh signaling within the dental epithelium is necessary for cell proliferation, growth and polarization, Development 129 (2002) 5323–5337.
[7] M.I. Cho, P.R. Garant, Development and general structure of the periodontium, Periodontology 2000 (24) (2000) 9–27.
[8] K.D. Kavanagh, A.R. Evans, J. Jernvall, Predicting evolutionary patterns of mammalian teeth from development, Nature 449 (2007) 427–432.
[9] Z. Zhang, Y. Lan, Y. Chai, R. Jiang, Antagonistic actions of Msx1 and Osr2 pattern mammalian teeth into a single row, Science 323 (2009) 1232–1234.
[10] J. Cai, S.W. Cho, J.Y. Kim, M.J. Lee, Y.G. Cha, H.S. Jung, Patterning the size and number of tooth and its cusps, Dev. Biol. 304 (2007) 499–507.
[11] J. Jernvall, I. Thesleff, Reiterative signaling and patterning during mammalian tooth morphogenesis, Mech. Dev. 92 (2000) 19–29.
[12] I. Salazar-Ciudad, J. Jernvall, A gene network model accounting for development and evolution of mammalian teeth, Proc. Natl. Acad. Sci. USA 99 (2002) 8116–8120.
[13] K. Nakao, R. Morita, Y. Saji, K. Ishida, Y. Tomita, M. Ogawa, M. Saitoh, Y. Tomooka, T. Tsuji, The development of a bioengineered organ germ method, Nat. Methods 4 (2007) 227–230.
[14] E. Ikeda, R. Morita, K. Nakao, K. Ishida, T. Nakamura, T. Takano-Yamamoto, M. Ogawa, M. Mizuno, S. Kasugai, T. Tsuji, Fully functional bioengineered tooth replacement as an organ replacement therapy, Proc. Natl. Acad. Sci. USA 106 (2009) 13475–13480.
[15] H.R. Dassule, P. Lewis, M. Bei, R. Maas, A.P. McMahon, Sonic hedgehog regulates growth and morphogenesis of the tooth, Development 127 (2000) 4775–4785.
[16] S. Kondo, A mechanistic model for morphogenesis and regeneration of limbs and imaginal discs, Mech. Dev. 39 (1992) 161–170.
[17] H.S. Jung, P.H. Francis-West, R.B. Widelitz, T.X. Jiang, S. Ting-Berreth, C. Tickle, L. Wolpert, C.M. Chuong, Local inhibitory action of BMPs and their relationships with activators in feather formation: implications for periodic patterning, Dev. Biol. 196 (1998) 11–23.
[18] Y. Litingtung, R.D. Dahn, Y. Li, J.F. Fallon, C. Chiang, Shh and Gli3 are dispensable for limb skeleton formation but regulate digit number and identity, Nature 418 (2002) 979–983.
[19] J. Jernvall, Linking development with generation of novelty in mammalian teeth, Proc. Natl. Acad. Sci. USA 97 (2000) 2641–2645.
[20] I. Salazar-Ciudad, J. Jernvall, A computational model of teeth and the developmental origins of morphological variation, Nature 464 (2010) 583–586.
[21] B. Hu, A. Nadiri, S. Kuchler-Bopp, F. Perrin-Schmitt, H. Peters, H. Lesot, Tissue engineering of tooth crown, root, and periodontium, Tissue Eng. 12 (2006) 2069–2075.
[22] R.I. Lechler, M. Sykes, A.W. Thomson, L.A. Turka, Organ transplantation – How much of the promise has been realized?, Nat Med. 11 (2005) 605–613.
[23] M.C. Raff, Size control: the regulation of cell numbers in animal development, Cell 86 (1996) 173–175.
[24] E. Ikeda, T. Tsuji, Growing bioengineered teeth from single cells: potential for dental regenerative medicine, Expert. Opin. Biol. Ther. 8 (2008) 735–744.

OPEN ACCESS Freely available online

PLoS one

Functional Tooth Regeneration Using a Bioengineered Tooth Unit as a Mature Organ Replacement Regenerative Therapy

Masamitsu Oshima[1☯], Mitsumasa Mizuno[1,2☯], Aya Imamura[3], Miho Ogawa[1,4], Masato Yasukawa[3], Hiromichi Yamazaki[3], Ritsuko Morita[1], Etsuko Ikeda[2], Kazuhisa Nakao[1], Teruko Takano-Yamamoto[2], Shohei Kasugai[5], Masahiro Saito[1,3], Takashi Tsuji[1,3,4]*

1 Research Institute for Science and Technology, Tokyo University of Science, Noda, Chiba, Japan, **2** Division of Orthodontics and Dentofacial Orthopedics, Graduate School of Dentistry, Tohoku University, Sendai, Miyagi, Japan, **3** Department of Biological Science and Technology, Graduate School of Industrial Science and Technology, Tokyo University of Science, Noda, Chiba, Japan, **4** Organ Technologies Inc., Tokyo, Japan, **5** Oral Implantology and Regenerative Dental Medicine Graduate School, Tokyo Medical and Dental University, Bunkyo-ku, Tokyo, Japan

Abstract

Donor organ transplantation is currently an essential therapeutic approach to the replacement of a dysfunctional organ as a result of disease, injury or aging *in vivo*. Recent progress in the area of regenerative therapy has the potential to lead to bioengineered mature organ replacement in the future. In this proof of concept study, we here report a further development in this regard in which a bioengineered tooth unit comprising mature tooth, periodontal ligament and alveolar bone, was successfully transplanted into a properly-sized bony hole in the alveolar bone through bone integration by recipient bone remodeling in a murine transplantation model system. The bioengineered tooth unit restored enough the alveolar bone in a vertical direction into an extensive bone defect of murine lower jaw. Engrafted bioengineered tooth displayed physiological tooth functions such as mastication, periodontal ligament function for bone remodeling and responsiveness to noxious stimulations. This study thus represents a substantial advance and demonstrates the real potential for bioengineered mature organ replacement as a next generation regenerative therapy.

Citation: Oshima M, Mizuno M, Imamura A, Ogawa M, Yasukawa M, et al. (2011) Functional Tooth Regeneration Using a Bioengineered Tooth Unit as a Mature Organ Replacement Regenerative Therapy. PLoS ONE 6(7): e21531. doi:10.1371/journal.pone.0021531

Editor: Wei-Chun Chin, University of California, Merced, United States of America

Received April 8, 2011; **Accepted** May 30, 2011; **Published** July 12, 2011

Funding: This work was partially supported by Health and Labour Sciences Research Grants from the Ministry of Health, Labour, and Welfare (No. 21040101) to T.T., a Grant-in Aid for Scientific Research in Priority Areas (No. 50339131) to T.T., a Grant-in-Aid for Scientific Research (A) to T.T. and a Grant-in-Aid for Young Scientists (B) to M. Oshima from Ministry of Education, Culture, Sports and Technology, Japan. The funders had no role in study design, data collection and analysis, decision to publish, or preparation of the manuscript.

Competing Interests: The authors have declared that no competing interests exist.

* E-mail: t-tsuji@rs.noda.tus.ac.jp

☯ These authors contributed equally to this work.

Introduction

Donor organ transplantation is currently essential to replace a dysfunctional organ and to restore organ function *in vivo* [1,2]. This approach is problematic for clinicians however as donor organs are constantly in short supply [2,3]. An attractive new concept in current regenerative therapy that may possibly replace conventional transplantation in the future is stem cell transplantation therapy [4,5] or a two-dimensional uniform cell sheet technique [6,7] to repair the local sites of the damaged tissues and organs [8]. The ultimate goal of regenerative therapy in the future is to develop organ replacement regenerative therapies that will restore lost or damaged tissues following disease, injury, or aging with a fully functioning bioengineered organ [9,10,11]. To construct a bioengineered organ, one of two major concepts is to construct fully functional artificial organs using three-dimensional tissue-engineering technology, involving biodegradable materials and various cell types, that can immediately function after transplantation *in vivo* [12,13,14]. However, further technological developments are required to create such artificial organs which can immediately function [15].

For the regeneration of ectodermal organs such as a tooth, hair follicle or salivary gland [16,17], a further concept has been proposed in which a bioengineered organ is developed from bioengineered organ germ by reproducing the developmental processes that take place during organogenesis [11,18]. Tooth regenerative therapy is thought to be a very useful study model for organ replacement therapies [11,19,20]. The loss of a tooth causes fundamental problems in terms of oral functions, which are achieved in harmony with the teeth, masticatory muscles and the temporomandibular joint under the control of the central nervous system [21]. It has been anticipated that a bioengineered tooth could restore oral and physiological tooth functions [19]. We have previously developed a three-dimensional cell manipulation method, designated the organ germ method, for the reconstitution of bioengineered organ germ, such as a tooth or whisker follicle [22]. This bioengineered tooth erupted with the correct structure, occluded at the lost tooth region in an adult mouse. It also showed sufficient masticatory performance, periodontal functions for bone remodeling and the proper responsiveness to noxious stimulations [20]. This previous study thus provided a proof of concept that

successful replacement of an entire and fully functioning organ could be achieved through the transplantation of bioengineered organ germ i.e. a successful organ replacement regenerative therapy [20].

Transplantation of a bioengineered mature organ will lead to immediately perform of the full functions *in vivo* and have a profound impact on the survival outcomes of many diseases [2,9]. Transplanted bioengineered organs are also expected to be viable over the long-term and achieve the continuous production of various functional cells and their progenitors from stem cells as efficiently as the natural organ *in vivo* [23,24]. It has also been proposed that mature organs can be developed from bioengineered organ germ by faithfully reproducing *in vivo* developmental processes. In the dental treatment, it has been expected to transplant of a bioengineered tooth unit comprising mature tooth, periodontal ligament (PDL) and alveolar bone into the tooth loss region through bone integration, which is connected between recipient bone and bioengineered alveolar bone in a bioengineered tooth unit [25]. Transplantation of a bioengineered tooth unit has also been proposed as a viable option to repair the large resorption defects in the alveolar bone after tooth loss [26]. However, there are currently no published reports describing successful transplantation or replacement using a bioengineered tooth [10,27].

In our current study, we have generated a bioengineered tooth unit, which was controlled for length and shape and report a successful tooth replacement by transplantation of a bioengineered tooth unit into the tooth loss region, followed by successful bone integration, and restoration of tooth physiological functions such as mastication, PDL function and an appropriate responsiveness to noxious stimulations. This transplantation of a bioengineered tooth unit could also regenerate alveolar bone formation in a vertical direction. Our results thus further demonstrate the potential for bioengineered tooth replacement as a future regenerative therapy.

Results

Generation of a Bioengineered Tooth Unit

We have previously reported that bioengineered tooth germ can successfully develop a bioengineered tooth that by subrenal capsule transplantation can restore a mature tooth, including periodontal tissue and alveolar bone [22]. Because a three-dimensional *in vitro* organ culture has not yet been developed, we employed a strategy involving a bioengineered tooth unit, which has the necessary tissues to restore tooth functions, to investigation and advance the future potential of bioengineered tooth replacement (figure 1A). The bioengineered molar tooth germ was developed to a stage equivalent to the early bell stage of natural tooth germ for 5–7 days in an *in vitro* organ culture (figure 1B). Although we have previously reported that multiple bioengineered teeth have been formed from a bioengineered tooth germ reconstituted by our organ germ method [22], we recently developed a method to generate a single and width-controlled bioengineered tooth [28]. The bioengineered tooth germ gradually accumulated hard tissue, root extension, and an increased alveolar bone volume, depending on transplantation periods, and could successfully generate a tooth unit with the correct structure of a whole molar, and the proper formation of periodontal tissue and surrounding alveolar bone (figure 1C, D). However, the shape (x vs. y axis) of the bioengineered tooth unit was flattened by the pressure of the outer membrane of the subrenal capsule (figure 1F, G). The length of the tooth also showed continuous root elongation depending on the transplantation periods without occlusional mechanical stress (figure 1C, F, H).

To generate the shape- and length-controlled bioengineered tooth unit so that a suitable size was obtained for intraoral transplantation, the tooth germ was inserted into a ring-shaped size-control device and then transplanted into a subrenal capsule (figure 1E). The crown widths, calculated from the x/y axis ratios, of natural first, second and third molars of 9-week-old adult mice were 1.61±0.05 mm, 1.09±0.04 mm, 1.12±0.04 mm, respectively (each n = 5, figure 1G). The crown width of the bioengineered tooth units grown in the size-control device, which had a 1.8 mm inside diameter and 1.3 mm thickness, was 1.46±0.16 mm whereas when grown outside of the device the size was 2.30±0.35 mm (each n = 5, figure 1G). The device thus successfully generated a size-controlled bioengineered tooth so that it was similar to a natural tooth (figure 1F, G). This device could avoid the pressure by the subrenal capsule membrane, and reserve the three-dimensional space for developing a bioengineered tooth germ normally. We next evaluated the length of a bioengineered tooth unit generated in the size-control device (figure 1E). After 30 or 60 days, the lengths of the teeth transplanted without the devices were 1.07±0.20 mm and 1.70±0.26 mm, respectively, which was significantly associated with the transplantation period (each n = 5, figure 1H, figure S1A). Although the length of the bioengineered tooth transplanted without the devices was 1.70±0.26 mm after 60 days transplantation, bioengineered teeth transplanted in devices of 1.3 or 1.8 mm in diameter, was significantly regulated at 1.02±0.11 or 1.27±0.06 mm, respectively (each n = 5, figure 1H). The shape and length of the bioengineered tooth unit can therefore be controlled in three-dimensions using a specialized device.

Multiple bioengineered tooth units surrounded by alveolar bone could be also generated by the transplantation of several tooth germs into a single size-control device (figure 1I, figure S1B). Each resulting tooth had the correct structure including pulp cavities and partitioned periodontal spaces (figure 1I, figure S1C). Hence, multiple tooth replacements can be achieved with this regenerative transplantation method.

Transplantation of a Bioengineered Tooth Unit into a Tooth Loss Region *in Vivo*

We next investigated whether a bioengineered tooth unit could be engrafted via the integration between the alveolar bone of this unit and that of the host recipient and then function appropriately by occlusion with an opposing tooth (figure 2A). The bioengineered tooth unit, which was generated by transplantation in a device of a 2.5 mm inside diameter for 50–60 days and labeled by the administration of calcein reagent into recipient mouse (figure 2B), was transplanted with the correct orientation into a properly-sized bony hole in the lower first molar region of the alveolar bone in a 4-week-old mouse (figure 2C). Briefly, in this mouse model, the lower first molar had been extracted, and the resulting gingival wounds had been allowed to heal for 4–6 days (figure S2A). When the bioengineered tooth unit was transplanted, it was located at a position reaching the occlusal plane with the opposing upper first molar (figure 2C, figure S2A). Partial bone integration was observed at 14 days after transplantation, and full bone integration around a bioengineered tooth root was seen at 30 days after transplantation (figure 2C). In the calcein-labeled alveolar bone of bioengineered tooth unit, resorption was partially observed at the surface at 30 days post-transplantation (figure 2D, figure S2B). The calcein-labeled bone finally disappeared and the recipient bone around the bioengineered tooth root replaced it completely at 40 days after transplantation at a frequency of 66/83 (79.5%; figure 2C, D, figure S2B). There have been many previously reported clinical cases of multiple tooth loss, the most serious condition being edentulism [29]. It is possible that a

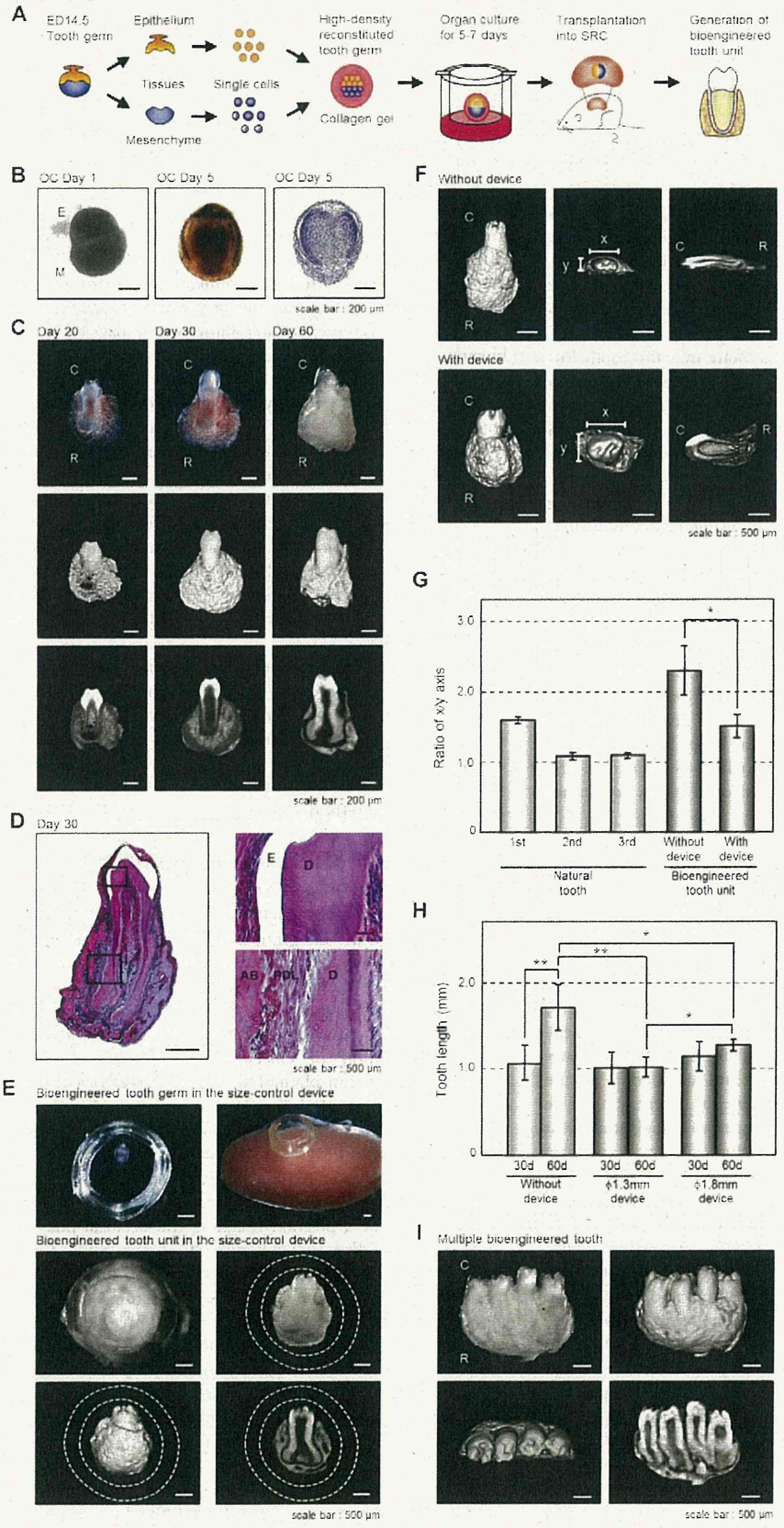
A
ED14.5 Tooth germ
Epithelium
Tissues
Mesenchyme
Single cells
High-density reconstituted tooth germ
Collagen gel
Organ culture for 5-7 days
Transplantation into SRC
Generation of bioengineered tooth unit
B
OC Day 1
OC Day 5
OC Day 5
scale bar : 200 μm
C
Day 20
Day 30
Day 60
scale bar : 200 μm
D
Day 30
scale bar : 500 μm
E
Bioengineered tooth germ in the size-control device
Bioengineered tooth unit in the size-control device
scale bar : 500 μm
F
Without device
With device
scale bar : 500 μm
G
Ratio of x/y axis
1st
2nd
3rd
Without device
With device
Natural tooth
Bioengineered tooth unit
H
Tooth length (mm)
30d
60d
Without device
φ1.3mm device
φ1.8mm device
I
Multiple bioengineered tooth
scale bar : 500 μm

Figure 1. Generation of a bioengineered tooth unit. (A) Schematic representation of the generative technology of bioengineered tooth unit. (B) Phase construct imagery of a bioengineered tooth germ on day 1 (*left*) and 5 (*center*) and HE staining (*right*) of an organ culture on day 5. Scale bar, 200 μm. E, epithelium; M, mesenchyme. (C) Photographs (*upper*) and micro-CT images of the external surface area (*middle*) and cross section (*lower*) of a bioengineered tooth unit. Images were captured at 20 days (*left*), 30 days (*center*) and 60 days (*right*) after subrenal capsule transplantation (SRC). Scale bar, 200 μm. C, tooth crown side; R, tooth root side. (D) Histological analysis of the bioengineered tooth unit on day 30 after SRC transplantation (*left*). (Scale bar, 500 μm). Higher magnification images of crown area (*upper right*) and the periodontal tissue area (*lower right*) are also shown. Scale bar, 50 μm. E, enamel; D, dentin; AB, alveolar bone; PDL, periodontal ligament. (E) Photographs of the developmental processes occurring in bioengineered tooth germ in a subrenal capsule (SRC) using a size-control device. Images were captured of bioengineered tooth germ orientated in the device (*top left*), transplantation into the SRC (*top right*), and the bioengineered tooth at 50–60 days after transplantation in the SRC (middle). Micro-CT images of the external surface area (*bottom left*) and cross section (*bottom left*) are also show. The dotted lines indicate the outlines of the device. Scale bar, 500 μm. (F) Micro-CT images of a bioengineered tooth unit transplanted into the SRC for 30 days with (*lower column*) or without (*upper column*) the size-control device at an external (*left*), axial (*center*) or cross section (*right*) view. Scale bar, 500 μm. x, x-axis of the crown; y, y-axis of the crown. (G) X-axis versus y-axis ratios (x/y) of the crowns of bioengineered tooth units at 30 days post transplantation into an SRC, and also of natural first, second and third molars from 9-week-old mice. Transplantations were performed with or without the 1.3 mm thickness size-control device. Error bars show the standard deviation ($n=5$). *$P<0.001$ (*t*-test). (H) The lengths of the bioengineered tooth units generated using size-control devices, which were of a 1.3 mm (φ1.3 mm) or 1.8 mm (φ1.8 mm) inner diameter, at 30 and 60 days post transplantation into an SRC were compared with or without the devices. Error bars show the standard deviation ($n=5$). *$P<0.01$ and **$P<0.001$ (*t*-test). (I) Photograph (*first figure from the left*) and micro-CT images showing external (*second figure*), axial (*third figure*) and cross section (*fourth figure*) views of a multiple bioengineered tooth units, in which four teeth were contained in one alveolar bone, after 60 days transplantation into the SRC. Scale bar, 500 μm.
doi:10.1371/journal.pone.0021531.g001

bioengineered teeth unit could be transplanted into an edentulous jaw (figure S2E, F). Our current findings suggest that bioengineered teeth can be engrafted into regions of tooth loss through bone integration, which involves resorption of the alveolar bone of the bioengineered tooth unit through natural bone remodeling in the recipient.

The engrafted bioengineered tooth was found to be aligned appropriately and occlude with the opposing upper first molar (figure 2E, figure S2C). Micro-CT analysis also revealed that no root elongation was evident for the bioengineered tooth and that the apical foramen of the engrafted bioengineered tooth root significantly narrowed at 40 days after transplantation (each n = 9, figure S2D). These results suggest that the bioengineered tooth in the tooth unit isolated from subrenal capsule transplantation is immature tooth, which has the potential to narrow of the apical foramen after the oral transplantation and would have the physiological ability to recapitulate mechanical stress by occlusion.

Masticatory potential is essential for proper tooth function and we next performed a Knoop hardness test, an important measure of masticatory functions, on bioengineered teeth including both the dentin and the enamel components. The Knoop hardness numbers (KHN) of the enamel and dentin in the natural teeth of 11-week-old adult mice were measured at 404.2±78.2 and 81.0±11.5, respectively (each n = 5, figure 2F). The bioengineered teeth generated in a subrenal capsule (SRC) and in jaw bone (TP) showed similar KHN values at 179.6±49.2 and 319.6±78.3 in the enamel, and 80.7±11.5 and 76.8±13.6 KHN in the dentin, respectively (each n = 5, figure 2F). The value of enamel Knoop hardness of natural tooth increase in according to postnatal period [20]. Although the enamel hardness of the bioengineered tooth generated in a SRC showed low KHN values, the enamel hardness of the engrafted bioengineered teeth (TP) increased to the high KHN value in according to the period after the transplantation into jaw bone. Therefore, the hardness of the dentin in the engrafted bioengineered teeth was in the normal range. These findings indicate that the hardness of the enamel and dentin in the engrafted bioengineered teeth were in the normal range.

Functional Analysis of the Periodontal Ligament and Neurons of the Engrafted Bioengineered Teeth

Previously, it had been demonstrated that the bioengineered tooth germ can recapitulate physiological tooth function in the adult murine oral environment [20]. In our present study, we next investigated whether an engrafted bioengineered mature tooth unit can also restore physiological tooth functions *in vivo* such as the response to mechanical stress and the perceptive potential for noxious stimulations. It is essential for tooth functions that the engrafted bioengineered tooth in recipient has the cooperation with the oral and maxillofacial regions through the PDL. The response of the PDL to mechanical stress, such as orthodontic movements, induces alveolar bone remodeling, which is indicated by the localization of tartrate-resistant acid phosphatase (TRAP)-osteoclasts and osteocalcin (*Ocn*) mRNA-positive osteoblasts [20]. During experimental tooth movement, TRAP-positive osteoclasts and *Ocn* mRNA-positive osteoblasts were observed on the compression and tension sides, respectively (figure 3A). This demonstrated that the PDL of the bioengineered tooth unit successfully mediates bone remodeling via the proper localization of osteoclasts and osteoblasts in response to mechanical stress.

The perceptive potential for noxious stimulation including mechanical stress and pain, are important for proper tooth function [30]. Trigeminal ganglional neurons, which innervate the pulp and PDL, can respond to these stimulations and transduce the perceptions to the central nervous system. Blood vessels that are detected in the pulp and PDL, maintain dental tissues such as odontoblasts, pulp, the PDL and alveolar bone. In our current experiments, we evaluated the responsiveness of nerve fibers in the pulp and PDL of the engrafted bioengineered tooth to noxious stimulations. Although von Willebrand Factor (vWF)-positive blood vessels were observed in the pulp and PDL of the bioengineered tooth generated in a subrenal capsule, anti-neurofilament (NF)-immunoreactive nerve fibers could not be detected (figure 3B, figure S3A, B). However, NF-positive nerve fibers could be detected in the pulp and PDL of the engrafted bioengineered tooth in the recipient bone and the neurons merged with vWF-positive blood vessels (figure 3B). Neuropeptide Y (NPY) and calcitonin gene-related peptide (CGRP), which are synthesized in sympathetic and sensory nerves, respectively, were also detected in both the pulp and PDL neurons (figure 3B, figure S3C–F). We found in our current analyses that c-Fos immunoreactive neurons, which are detectable in the superficial layers of the medullary dorsal horn following noxious stimulations such as mechanical and chemical stimulation of the intraoral receptive fields, were present in both normal and bioengineered teeth and drastically increased in number at two hours after orthodontic treatment and pulp exposure (figure 3C). These results indicate that an engrafted bioengineered tooth unit can indeed restore the

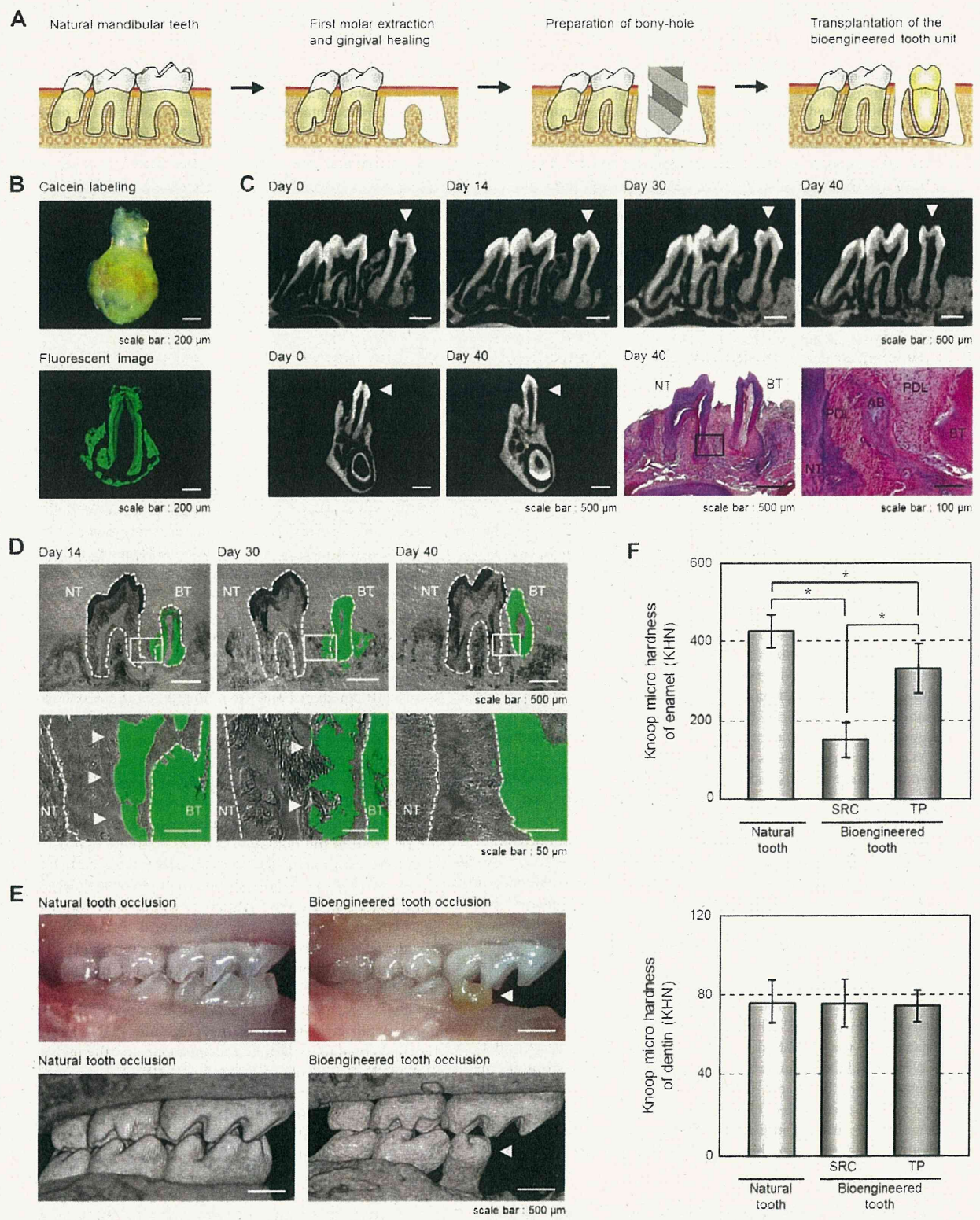

Figure 2. Engraftment and occlusion of a bioengineered tooth unit in a tooth loss model. (A) Schematic representation of the protocol used to transplant a bioengineered tooth unit in a murine tooth loss model. (B) Photograph (*Upper*) and sectional image (*Lower*) of a calcein-labeled bioengineered tooth unit at 60 days post transplantation in an SRC. Scale bar, 200 μm. (C) Micro-CT images of a bioengineered tooth unit (arrowhead) in cross section (*upper*) and frontal section (*first and second figures from the lower left*) during the processes of bone remodeling and

connection between the recipient jaw bone and alveolar bone of the tooth unit. Histological analysis of the engrafted bioengineered tooth unit at 40 days post transplantation was also performed. (Scale bar, 500 μm and 100 μm in the lower and higher magnification figure; *third and fourth figure from the lower left*). NT, natural tooth; BT, bioengineered tooth; AB, alveolar bone; PDL, periodontal ligament. (D) Sectional images of a calcein-labeled bioengineered tooth unit at 14, 30 and 40 days post-transplantation. The calcein-labeled bone of the bioengineered tooth units (arrowhead) was found to gradually decrease from the outside and finally disappear at 40 days post-transplantation. Scale bar, 500 μm (*upper*), 50 μm (*lower*). NT, natural tooth; BT, bioengineered tooth. (E) Oral photographs (*upper*) and micro-CT (*lower*) images showing occlusion of natural (*left*) and bioengineered teeth (*right*). Scale bar, 500 μm. (F) Assessment of the hardness of a bioengineered tooth. Knoop microhardness values of the enamel (*upper*) and dentin (*lower*) of a bioengineered tooth at 60 days post-transplantation in a subrenal capsule (SRC) and at 40 days post-transplantation in jawbone (TP) were compared with those of natural teeth in 11-week-old mice. Error bars show the standard deviation ($n = 5$). *$P<0.01$ (*t*-test).
doi:10.1371/journal.pone.0021531.g002

perceptive potential for noxious stimulations in cooperation with the maxillofacial region.

Regeneration of an Extensive Bone Defect by Transplantation of a Bioengineered Tooth Unit

Tooth loss is well known to cause significant alveolar bone resorption at the region in question [26]. Although there have been many studies of bone regenerative therapies [31], more effective methods to restore extensive bone defects during treatments such as dental implants are required and anticipated [26]. We investigated whether the transplantation of a bioengineered tooth unit would regenerate not only the missing tooth but also the surrounding alveolar bone of the recipient. To analyze whether such restoration of the alveolar bone occurred after transplantation, we developed a murine extensive bone defect model, which was prepared by the extraction of the lower first molar and then removal of the surrounding alveolar bone to generate a critical bone defect in the lower first molar region (figure 4A, figure S4A). When we transplanted a bioengineered tooth unit into this bone defect, vertical bone formation was observed from the marginal bone of the recipient at 14 days after transplantation (figure 4B, C, figure S4B). The regenerative bone volume post-transplantation significantly increased compared with a no transplant control (0.38 ± 0.07 mm^3 vs. 0.12 ± 0.08 mm^3; each $n = 4$, figure 4C, D), although the height and volume of the regenerated alveolar bone surrounding the bioengineered teeth was not completely recovered. These findings indicate that transplantation of a bioengineered tooth unit can restore a serious bone defect.

Discussion

We here demonstrate the successful transplantation of a bioengineered tooth unit, which is a model for a bioengineered mature organ, into a missing tooth region *in vivo* and the subsequent restoration of tooth function by this graft. We also show that this transplantation can restore the bone volume in both the vertical and horizontal dimensions in a missing tooth mouse model with a serious extensive bone defect. These findings indicate that whole tooth regenerative therapy is feasible through the transplantation of a bioengineered mature tooth unit. This study also provides the first reported evidence of entire organ regeneration through the transplantation of a bioengineered tooth.

Organ replacement regenerative therapy, but not stem cell transplantation regenerative therapy for tissue repair, holds great promise for the future replacement of a dysfunctional organ with a bioengineered organ reconstructed using three-dimensional cell manipulation *in vitro* [11,19]. In previous reports, however, artificial organs, which were constructed with various cells and artificial materials could not restore functionality and thus are not a viable option for long-term organ replacement *in vivo* [15]. Previously, it has been shown that a bioengineered organ can be grown *in vivo* in amphibian models in which activin-treated cell aggregates could form a secondary heart with pumping function and also regenerate eyes that were light responsive and connected with the host nervous system [32,33]. Recently, we have also regenerated bioengineered organ germs, including tooth germs and whisker follicles, and successfully achieved a fully functioning tooth replacement in an adult mouse through the transplantation of a bioengineered tooth germ in the lost tooth region [20,22]. It has been anticipated that replacement therapies will be developed in the future through the transplantation of a bioengineered mature organ with full functionality and long-term viability [2,19]. In our present experiments, we successfully generated a size-controlled bioengineered mature tooth unit, a strategy we adopted because the growth of functional organs *in vitro* is not yet possible [27]. Organs require a sufficient mass (cell number) and proper shape to function [34] and the tooth has unique morphological features, such as the tooth crown width and length (macro-morphology), and cusp and root shape (micro-morphology) [35]. However, the technology to regulate tooth morphogenesis for whole tooth regeneration remains unexplored [36]. We recently developed a novel organ germ method to regulate the crown width by regulating the contact area between epithelial and mesenchymal cell layers [28]. In our previous work, we demonstrated that the length of the bioengineered tooth is equivalent to that of natural tooth after the transplantation of the bioengineered tooth germ into oral environment [20]. In this study, the length of the bioengineered tooth unit could be controlled longitudinally, which would be provided by the limited space of the device. These findings provide the first evidence that the bioengineered tooth can be controlled in three-dimensions using a specialized device. It is also thought that bioengineered teeth could be generated with a controlled crown width through cell manipulation and tooth length by placement in a size-controlling device, which places a three-dimensional spatial limitation on size [20,28].

Loss of teeth and functional disorders in the PDL or temporomandibular joint, cause fundamental problems for oral functions, such as enunciation, mastication and occlusion, and associated health issues [21]. Although, missing teeth are traditionally restored by replacement with an artificial tooth, such as a bridge, denture or osseo-integrated dental implant, it is thought that the proper restoration of tooth functions will require bone remodeling regulated by the PDL [20] and a proper responsiveness to noxious stimulations [30]. Previous reports of autologous tooth transplantations have indicated that natural periodontal tissue on the tooth could restore the physiological tooth function, including bone remodeling [37]. We recently showed that a fully functional bioengineered tooth can be achieved through the transplantation of a bioengineered organ germ [20]. In our current study, we demonstrate the successful replacement of an entire and fully functional tooth unit *in vivo*, which restored masticatory potential, the functional responsiveness, including bone remodeling, of the periodontal tissue to mechanical stress and proper responsiveness to noxious stimulations via both peripheral sensory and sympathetic nerves. This is a significant

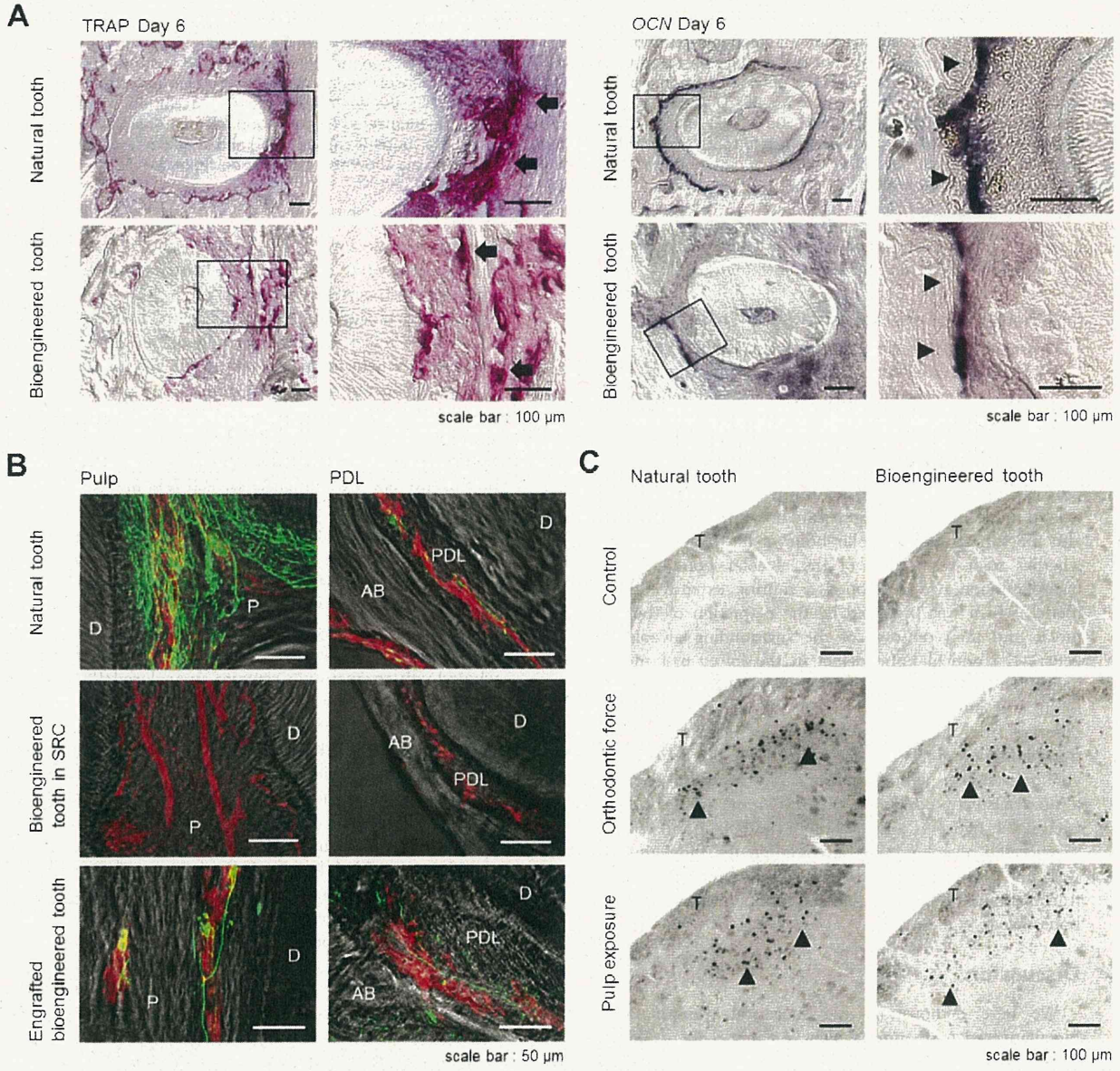

Figure 3. Experimental tooth movement and pain response to mechanical stress. (A) Sections of natural and bioengineered teeth were analyzed by TRAP-staining and *in situ* hybridization analysis of *Ocn* mRNA at day 6 of orthodontic treatment. TRAP-positive cells (arrow) and *Ocn* mRNA-positive cells (arrowhead) are indicated. Scale bar, 100 μm. (B) Nerve fibers and blood vessels in the pulp and PDL of a natural tooth (*top*), a bioengineered tooth unit in an SRC (*middle*), and a bioengineered tooth at 40 days after transplantation (*bottom*) were analyzed immunohistochemically using specific antibodies for neurofilament (NF; green) and von Willebrand Factor (vWF; red). Scale bar, 50 μm. D, dentin; P, pulp; AB, alveolar bone; PDL, periodontal ligament. (C) Analysis of c-Fos immunoreactive neurons in the medullary dorsal horns of mice after 0 hours (no stimulation, control; *top*), 2 hours of stimulation by orthodontic force (*middle*) and pulp exposure (*bottom*). C-Fos (arrowhead) was detectable after these stimulations in both natural (*left*) and bioengineered teeth at 40 days post-transplantation (*right*). Scale bar, 100 μm. T, spinal trigeminal tract.
doi:10.1371/journal.pone.0021531.g003

advance for the concept of whole tooth regenerative therapy in which the transplantation of a bioengineered mature organ, and not organ germ, can replace an organ and restore its full function.

In order for a tooth to cooperate with the maxillofacial region, it is supported by the connection between the root cementum and alveolar bone through the PDL, which has essential roles in tooth support, resorption and repair of the root cementum, and the remodeling of alveolar bone [38]. Tooth loss causes a large amount of alveolar bone resorption, which is mediated by the PDL, in the vertical and horizontal dimensions, and the loss of this bone, which leads to both functional and aesthetic problems, is difficult to rectify with standard dental therapies such as dental implant and autologous tooth transplantation [26]. Although bone regeneration has been attempted for many years through the use of tissue engineering technologies, guided bone regeneration methods, autologous bone or cell transplantation, and cytokine